Aus der Klinik für Gastroenterologie, Stoffwechselerkrankungen und Internistische

Intensivmedizin (Med. Klinik III)

Direktor Univ.-Prof. Dr. Christian Trautwein

JNK1 in Hepatic Stellate Cells is a crucial mediator of liver fibrogenesis in mice

Von der Medizinischen Fakultät der Rheinisch-Westfälischen Technischen Hochschule Aachen zur Erlangung des akademischen Grades eines Doktors der Medizin genehmigte Dissertation

vorgelegt von

Master of Medicine (Southeast University, Nanjing, China)

Gang Zhao

aus Anhui (China)

Berichter: Universitätsprofessor Dr. med Christian Trautwein

Universitätsprofessor Dr. rer. nat Ralf Weiskirchen

Tag der mündlichen Prüfung: 29.01.2013

Diese Dissertation ist auf den Internetseiten der Hochschulbibliothek online verfügbar.

Table of contents

1 Introduction

1.1 Liver anatomy and physiology..... 4

1.2 Liver fibrosis..... 5

1.2.1 Etiology and clinical signs of liver fibrosis..... 5

1.2.2 Pathophysiology of Liver Fibrosis..... 6

1.3 Hepatic Stellate Cells (HSCs) and liver fibrosis..... 7

1.4 Cell types involved in liver fibrosis..... 8

1.4.1 Portal fibroblasts 9

1.4.2 Bone marrow-derived cells (BMCs) 9

1.4.3 Epithelial-to-mesenchymal transition (EMT) 9

1.5 Current treatment of liver fibrosis..... 9

1.6 The JNK signaling pathway..... 10

1.7 The role of JNK in liver injury..... 12

1.8 The function of JNK in liver fibrosis..... 13

1.9 Aim of the study..... 15

2 Material and Methods

2.1 Materials

2.1.1 Chemicals..... 16

2.1.2 Standard buffer and media..... 18

2.1.3 Standard kits and enzymes..... 19

2.1.4 Antibodies used for immunostaining and/or Western Blot..... 19

2.1.5 Primer sequences used for qRT-PCR..... 20

2.1.6 Primer sequences used for genotyping (PCR) 21

2.1.7 Instruments and other equipment..... 21

2.2 Methods

2.2.1 Bile duct ligation (BDL) 23

2.2.2 Bone marrow transplantation (BMT) 23

2.2.3 Isolation of HSCs with FACS sorting..... 24

2.2.4 Microarray Analysis..... 25

2.2.5 Housing and breeding of mice..... 25

2.2.6 Induction of liver fibrosis in mice..... 25

2.2.7 Genotyping..... 26

2.2.8 Blood sampling and serology..... 27
2.2.9 Liver perfusion and isolation of primary hepatocytes..... 27
2.2.10 RNA extraction, cDNA preparation, qRT-PCR..... 28
2.2.11 Protein concentration measurement..... 29
2.2.12 Western Blot 30
2.2.13 Immunofluorescence staining (IF) 31
2.2.14 Immunohistochemistry (IHC) 31
2.2.15 Statistical analysis..... 32
3 Results
3.1 JNK1 in hepatocytes has no impact on hepatic injury during experimental liver fibrosis..... 33
3.2 non-parenchymal cells (NPCs) JNK1 determines hepatocyte proliferation after BDL and CCl_4 treatment..... 37
3.3 JNK1 in NPCs promotes liver fibrogenesis..... 40
3.4 The WT recipient genotype after BMT determines the degree of liver injury..... 44
3.5 JNK1 in BMCs has no relevance for liver fibrosis..... 47
3.6 Array analysis suggests that genes involved in matrix formation are decreased in $Jnk1^{-/-}$ mice..... 49
3.7 JNK1 is essential for HSCs transdifferentiation..... 52
4 Discussion
4.1 The contribution of JNK1 in hepatocytes and NPCs to chronic liver injury 57
4.2 The role of JNK1 in hepatocytes and NPCs to liver fibrosis..... 58
4.3 The analysis of the function of JNK1 in BMCs during liver injury..... 60
4.4 Assess the role of JNK1 in HSCs *in vivo* and *in vitro*..... 61
5 Summary 63
6 Zusammenfassung 64
7 References 66
8 Appendix
Abbreviations..... 72
Publications..... 75
Eidesstattliche Erklärung..... 76

Erklärung..... 77
Acknowledgements..... 78
Curriculum vitae..... 80

1. Introduction

1.1 Liver anatomy and physiology

The liver, the second largest organ of the human body, weights about 1500 g. It is located in the right upper quadrant abdominal cavity of the human body[1]. The liver is a vital organ and plays a major role in energy metabolism, which includes proteins related to synthesis, enzymes and cofactors, digestion, and the regulation of metabolic functions. Moreover, the liver is involved in the regulation of the body's protein, fat and carbohydrate metabolism, transformation, biliary excretion, and metabolism of toxic compounds and drugs[2]. As the first line of defence against ingested toxins and many infectious agents, the liver has evolutionarily conserved responses including the ability to regenerate and to protect itself against injury.

The liver is composed of hepatic lobules constituted by parenchymal cells (hepatocytes and cholangiocytes) and non-parenchymal cells (NPCs) (Figure 1). Hepatocytes are the most numerous cells of the liver, represent 80% of total volume of the liver cells and the number accounted for about 60%[3]. NPCs numbers account for 40% of the total number of liver cells, but only 6.5% to the total liver volume, are localized in the sinusoidal compartment of the liver. Sinusoidal endothelial cells (SECs), Kupffer cells (KCs), hepatic stellate cells (HSCs), lymphocytes and oval cells are some of the NPCs that constitute the hepatic sinusoid[3]. SECs are fenestrated endothelium surrounding the sinusoids of the liver. They possess flattened shape and are united through adherent junctions. SECs have numerous vesicles in the cytoplasm and nuclei located in the center of the cell. The perforation between these cells is very large, which average diameter is about 100 μm, so that blood can easily come into contact with the hepatocytes microvilli through the space of Disse. KCs, which are the macrophages of the liver, are monocytes located in the lumen of the venous sinusoids. The numerous protrusions typical of cells of the macrophage, whose shape is variable and irregular, extend into the lumen of the sinusoid. Hepatic macrophages secrete potent inflammatory mediators and control the early phase of liver inflammation, playing an important part in innate immune defense. Moreover, during liver injury and inflammation, KCs secrete enzymes and cytokines that may damage hepatocytes and participate in the remodeling of ECM[4]. HSCs are placed

between the plates at the base of hepatocytes, and have a star-shaped or irregular. As the cells quiescent stage, their cytoplasm is rich in lipid vesicles containing vitamin A. During liver injury they become activated myofibroblasts with the lipid vesicles disappearing and produce ECM that lead to liver scarring and structural deformation, leading to the progression of liver fibrosis and injury[5]. Lymphocytes are also part of the innate immune system and help resist infection[4]. The oval cell is the liver-specific stem cell, a blast-like cell capable of self renewal and multipotent differentiation, which can only be identified in the setting of chronic liver injury when resident hepatocytes are unable to enter the cell cycle to restore liver mass. Evidence suggests that oval cells are bipotential, capable of differentiating into mature hepatocytes or cholangiocytes under different experimental conditions[6]. All these cell types are activated following hepatic injury[7].

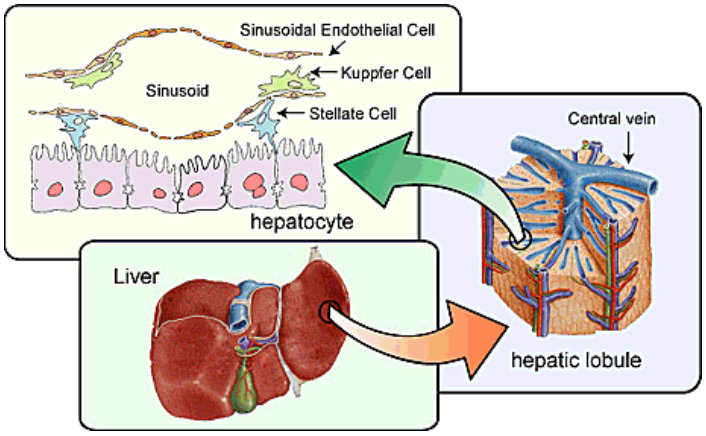

Figure 1. The liver is composed of hepatocyte (parenchymal cell) and NPC, such as KC, SEC, HSC. Hepatocytes adhere to each other via a junctional complex formed by a tight junction, an adherence junction, and a gap junction. These cell environment and cell-cell interactions contribute to maintenance of liver functions and liver regeneration. Courtesy of Akaike Laboratory; source: http://www.akaike-lab.bio.titech.ac.jp/akaike/english/resarch/index.html

1.2 Liver fibrosis

1.2.1 Etiology and clinical signs of liver fibrosis

The accumulation of ECM proteins during a long period results in the development of liver fibrosis[8]. The etiology of liver fibrosis in industrialized countries includes chronic HCV infection, alcohol abuse, and non-alcoholic steatohepatitis (NASH) or non-alcoholic fatty liver disease (NAFLD)[9]. Pathophysiology perspective, studies have shown that the accumulation of ECM distorts the hepatic architecture by

forming a fibrous scar. Hepatic fibrosis produces hepatocellular dysfunction and increased intrahepaticresistance to blood flow, which result in hepatic insufficiency and portal hypertension, respectively, and can trigger growth of hepatocellular carcinoma (HCC)[10].

1.2.2 Pathophysiology of liver fibrosis

Hepatic fibrosis is the result of the wound-healing response of the liver to prolonged injury[8]. After an acute liver injury (e.g., Drug-induced hepatitis), parenchymal cells regenerate and replace the necrotic or apoptotic cells. This process is associated with an inflammatory response and a limited deposition of ECM. If the hepatic injury persists, then eventually the liver regeneration fails, and hepatocytes are substituted with abundant ECM, including fibrillar collagen[9]. The distribution of this fibrous material depends on the origin of the liver injury. In cholestasis-induced liver fibrosis, the fibrotic tissue is initially located around portal tracts, while in alcohol-induced liver disease, it locates in pericentral and perisinusoidal areas[11]. As the disease progression of liver fibrosis, liver fibrosis is the major changes in the number and composition of the ECM, collagen band from bridging fibrosis to cirrhosis occurred[12]. In advanced stages, the liver contains about 6 times higher than the normal state, including collagens (I, III, and IV), fibronectin, elastin, laminin, hyaluronan, and proteoglycans. Accumulation of ECM results from both increased synthesis and decreased degradation. Declined activity of MMPs (matrix metalloproteinases), which is responsible for the elimination of ECM, mainly due to an overexpression of their specific inhibitors (TIMPs)[13].

With the widespread use of the mouse models of hepatic fibrosis, extensive studies have revealed key gene-mediated hepatic fibrogenesis[14]. Genes regulating hepatocellular apoptosis and/or necrosis (e.g. TNF-R1, FasR and DR5) influence the extent of hepatic damage and the subsequent fibrogenic response[15-16]. Genes regulating the inflammatory response after injury (e.g., IL-1β, IL-6, IL-10, and IL-13, IFN-γ, SOCS-1, and OPN) determine the fibrogenic response to injury[17-19]. In addition, genes mediating ROS generation (e.g. catalase) regulate the progression of liver fibrosis[20-21].

1.3 HSCs and liver fibrosis

HSCs are normally quiescent cells and show a star-like appearance. When HSC is activated, they undergo excessive cellular proliferation and transdifferentiate into myofibroblasts which have a high degree of contractility[22]. Quiescent HSCs represent 5-8% of the total number of liver cells. They play a key role in storage and controlled release of retinoids[22]. The most characteristic structural feature of quiescent HSCs is the presence of numerous, large cytoplasmic lipid droplets, which are composed of retinoids, triglycerides, cholesterol and FFA[5]. Based on the presence of vitamin A, HSCs encompass an autofluorescence under the UV light radiation and can be distinguish their identification. In the normal liver, HSCs include diverse functions. As localization within the space of Disse, HSCs are proposed to be the key cell type that regulates hepatic blood flow and pressure[23]. In addition, studies have shown that the HSCs capable of expressing a variety of receptor proteins and secreted proteins that include receptors for ECM components, cytokines, growth factors, chemokines, vasoactive substances and several other ligands[24]. Moreover, HSCs are considered to serve as a hepatic progenitor cell and are essential in balancing the MMP/TIMP system[25].

When cultured on a plastic dish with the fetal calf serum, HSCs are easy attachment, proliferation, and spontaneous transdifferentiation. This phenomenon is as similar as observed with chronic liver diseases of HSC activation process. During this process, HSCs increase the expression of characteristic markers including α-SMA and collagen type I that are considered to be indispensable event in the pathogenic sequence of fibrogenesis. The resulting phenotype produces a large variety of ECM indicative for fibrotic connective tissue and expresses a sundry of cytokines and chemokines triggering the fibrogenic response[26]. Activated HSCs express desmin and GFAP, PDGF, TGF-β and several other cytokines, as well as oxidative stress and lipid peroxidation products fuel the process of transdifferentiation[27]. The transdifferentiation process will further exacerbate by paracrine-acting mediators released from liver cells, for example hepatocytes, KCs and SECs, and from invading non-hepatic cells, such as platelets, lymphocytes and leukocyte subtypes[28].

Activation of HSCs in culture resembles its *in vivo* activation after chronic liver injury[5]. In comparison to their quiescent counterpart, they have a different gene-

expression profile that particularly affects growth factors, nuclear receptors, cytoskeleton proteins and their receptors, cytokines and chemokines. Moreover, they change their morphology, their cellular ultrastructure, acquire contractile properties on a variety of cytokines and chemokines[29].

Animal models of liver fibrosis, such as CCl_4 treatment or surgical bile duct ligation (BDL) surgery, clearly show the role of HSC in liver fibrosis. In pathological conditions such as liver fibrosis, the phenotypic changes related with myofibroblastic transdifferentiation is a reduction of lipid droplets, loss of stored vitamin A, increased synthesis of collagen and α-SMA, reorganisation of the actin cytoskeleton, increased deposition of ECM and proliferation[30-31]. Recent studies using murine models of hepatic fibrosis have revealed a close interaction between inflammatory signals, monocytes/macrophages and HSCs for the initiation of fibrogenesis *in vivo*[5]. Actually, HSCs activation is driven by TNFα and other cytokines together with KCs. HSCs can be activated via TLR4 by various sources of bacterial lipopolysaccharide (LPS), such as that originating from intestinal flora. Activated HSCs produce chemokines that include MCP-1 or RANTES[32]. The release of these chemokines attracts monocytes from the peripheral blood into the injured liver. Infiltrating monocytes rapidly differentiate into inflammatory macrophages in the liver that produce a large number of TGF-β, which is the main factor stimulating HSCs activation[33]

1.4 Cell types involved in liver fibrosis

In the process of liver fibrosis, many experiments confirmed that collagen-producing myofibroblasts are mainly derived from HSCs *in vivo*[34]. However, the following other cellular sources may contribute to ECM production in the liver as well (Figure 2).

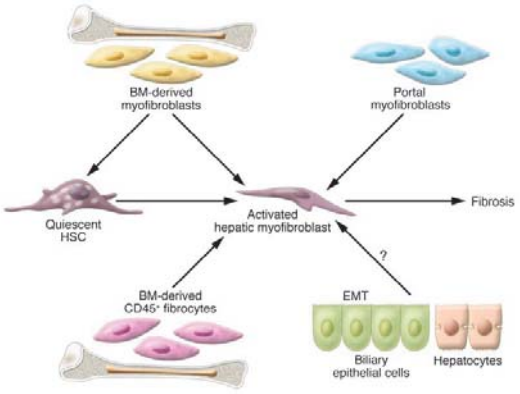

Figure 2. Sources of myofibroblasts in liver injury. Multiple sources of fibrogenic myofibroblasts are likely in liver injury depending on the site and nature of the injury. While resident HSCs appear to be the most likely source, periportal fibroblasts may be especially prominent in biliary injury, whereas BMCs and possible EMT may contribute as well. Courtesy of John P. Iredale[35].

1.4.1 Portal fibroblasts

These mesenchymal cells are considered to represent resident fibroblasts in the portal areas. Their activation may be especially important role to the liver fibrosis caused by cholestatic disease, which is characterized by a distribution in the portal tracts[36]. From the experimental evidence of cholestatic fibrosis model, portal fibroblasts can transdifferentiate into myofibroblasts following a pattern similar to the transdifferentiation of HSCs and further contribute to the fibrogenic process by triggering bile duct epithelia hyperproliferation[37].

1.4.2 Bone marrow-derived cells (BMCs)

Presently, there are two distinct populations of BMCs known that could contribute to hepatic fibrogenesis. The first group are bone marrow-derived mesenchymal stem cells. The second option is fibrocytes. Unfortunately, yet more light needs to be shed on this issue as these experimental studies have proven to show rather limitation and potential flaw and more research needs to verify the role of BMCs in liver fibrosis[38].

1.4.3 Epithelial-to-mesenchymal transition (EMT)

The EMT is an important process, which is characterized by a loss of cell adhesion function and repression of E-cadherin expression during embryonic development[38]. Recent studies indicated that EMT can be reactivated in pathological conditions and might thus represent a promising therapeutic target for the attenuation of liver fibrosis[39-40]. However, the concept of EMT has been severely argued among fibrosis researchers in recent years[40-41]. Thus, it is presently not clear if and to what extent EMT-related mechanisms contribute to liver fibrogenesis.

1.5 Current treatment of liver fibrosis

Several antifibrotic approaches exist. The removal of the causative agent is the most effective intervention in the treatment of liver fibrosis. This strategy has been proven to be effective in the etiologys of most chronic liver diseases[42]. For example, chronic HCV infection is the most extensively studied disease, and therapy (IFN-α

plus ribavirin) with viral clearance results in fibrosis remission. Importantly, nearly 50% of the patients with cirrhosis have significantly eased[42-43].

Another method is the inhibition of HSCs activation by modulating either their activation and/or proliferation or promoting their apoptosis. Antioxidants such as vitamin E and S-adenosyl-L-methionine (SAM) inhibit HSCs activation and attenuate experimental liver fibrosis[44]. Another molecule that does inhibit the HSCs activation is IFN-γ[45]. Furthermore, the use of synthetic ligands was tested for peroxisome proliferators activated nuclear receptors (PPAR). All of these receptors are present on the surface of HSCs and especially PPAR-γ seems to inhibit the activation of HSCs[46-47].

Because inflammation precedes and promotes the progression of liver fibrosis, the use of anti-inflammatory drugs has been proposed to inhibit the fibrogenesis. Moreover, since TNFα is one of the major pro-inflammatory cytokines such as antibodies, soluble TNF-R has been used and tested in mouse models of hepatitis[48].

In addition to the above methods, a direct antagonist of collagen expression and usage of growth factors were used to treat liver fibrosis[45]. Moreover, recently usage of mesenchymal stem cells might also be a possible approach to regenerate an established liver fibrosis[49-50]. Overall, finally remains that liver fibrosis can potentially be targeted by several strategies. Time will tell us which strategy - drug treatment, antagonist usage, gene therapy or a combination method will be the treatment of choice for liver fibrosis.

1.6 The JNK signaling pathway

C-Jun N-terminal kinase (JNK) is a member of the MAPK family. These proteins are serine-threonine protein kinases, which are activated in response to a variety of extracellular stimuli and mediate signal transduction from the cell surface to the nucleus. Three major MAPKs include ERKs, JNKs, and p38 kinases[51]. Ten JNK isoforms have been identified and are encoded by three distinct genes, JNK1, JNK2, and JNK3, the transcripts of which are alternatively spliced to yield four JNK1 isoforms, four JNK2 isoforms, and two JNK3 isoforms. JNK1 and JNK2 are the products of alternative splicing of a single gene and are expressed in almost all cells, including liver parenchymal cells, whereas JNK3 is mainly expressed in brain, heart, and testis[52-53].

JNKs are activated in response to stimuli such as inflammatory cytokines, bacterial products, oxidative stress, pathologic and environmental stress (ischemia, hypoxia, as well as UV and ionizing radiation), toxins, drugs, endoplasmic reticulum (ER) stress, and metabolic changes, including obesity and hyperlipidemia[52]. The upstream pathway leading to JNK activation is a complex process governed by different signaling proteins. Actually, JNK phosphorylation is mediated by two MAPK kinases (MAPKKs) - MKK4 and MKK7 - that can cooperatively activate JNK. JNK targets are cellular processes, regulating proliferation, cell death, inflammation, and metabolism and acting either as transcription factors or by controlling protein degradation, localization, and signaling (Figure 2). The substrates for JNK include c-Jun, JunB, JunD, AF2, p53, c-Myc, Itch, IRS-1, JIP-1, Bcl-2, Bcl-xL, Bid, Bim, Bad, Bax, and Mcl-1[51-52, 54].

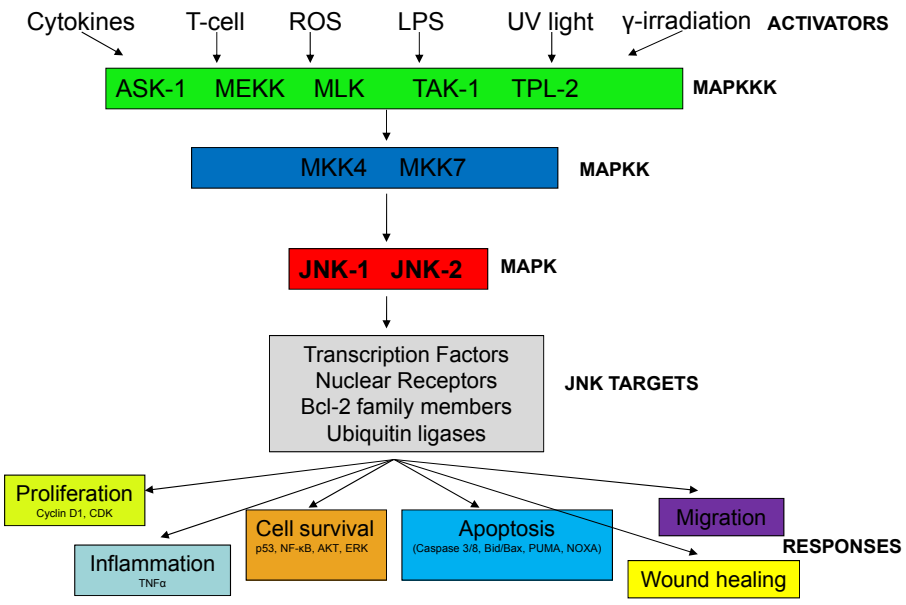

Figure 3. The JNK signalling pathway . Stress-activated protein kinases (SAPK)/JNK are members of the MAPK family and are activated by a variety of environmental stresses, inflammatory cytokines, ROS and LPS. The membrane proximal kinase is a MAPKKK that phosphorylates and activates MKK4 or MKK7, the SAPK/JNK kinases. SAPK/JNK translocates to the nucleus where it can regulate the activity of multiple transcription factors.

1.7 The role of JNK in liver injury

A role for JNK in apoptosis is well established and the mechanism by which this occurs is controversial and appears to be stimulus- and tissue-specific[55]. One explanation for some of the differences could be the temporal aspect of JNK activation[56]. Recent studies demonstrate that both the transient and sustained phases of JNK activation contribute to the induction of gene expression. However, early transient JNK activation promotes cell survival, whereas prolonged JNK activation can mediate apoptosis[52].

Several reports demonstrated that c-Jun – a crucial downstream target of JNK – is essential for liver regeneration as conventional c-Jun knockout animals die during embryonic development which has been linked to death of fetal liver cells[57]. In contrast, conditional hepatocyte-specific inactivation of c-Jun resulted in impaired hepatocyte proliferation during liver development and after partial hepatectomy[58]. Additionally, JNK inhibitors such as SP600125 have been used to study the relevance of JNK activation for liver regeneration[59]. These studies showed reduced hepatocyte proliferation during liver regeneration suggesting that JNK is necessary for liver regeneration.

Current research has demonstrated that JNK may also play important roles in other forms of cell death, including necrosis and autophagy. Ventura and colleagues have confirmed that JNK contributes to TNF-stimulated necrosis in cells when the NF-κB pathway is inhibited by promoting the production of cytotoxic ROS[60]. The anti-apoptotic proteins are phosphorylated by JNK *in vitro* and transfection studies indicate that this phosphorylation may suppress the antiapoptotic functions of these proteins[55].

A number of studies suggest that the JNK genes are functionally redundant in animal development and cell growth regulation. Both JNK1 and JNK2 are required for regional specific apoptosis of the brain in early development, neural tube morphogenesis and T cell proliferation[61]. Aside, emerging evidence suggests that the JNK genes may play different roles in many instances. Thus, it has been reported that JNK1, rather than JNK2, is involved in cell proliferation. However, JNK2 inhibits cell growth[62]. Some authors have considered a prominent role of JNK1, but not JNK2, during TNF-induced apoptosis *in vitro*[63] and *in vivo*[64]. Wang *et al*[65] have thought while JNK2 is essential for TNFα mediated apoptosis JNK1 is not directly involved in

this pathway. A possible explanation for these findings could be the different molecular targets of JNK1 and JNK2. JNK1 acts pro-apoptotic via Itch activation and subsequent c-FLIP degradation leading to low c-FLIP levels, reduced inhibition of caspase 8 and increased apoptosis. In turn, JNK2 directly mediates caspase 8 activation, via a yet unknown mediator[66].

1.8 The function of JNK in liver fibrosis

NAFLD is a hepatic manifestation of the metabolic syndrome, which is characterized by obesity and insulin resistance. The spectrum of NAFLD ranges from simple steatosis to steatosis with hepatic inflammation and fibrosis, known as NASH. NASH is a high risk factor for cirrhosis. Studies have shown interesting information of role of JNKs in fatty liver diseases. For example, research using HFD and MCD diet revealed that the JNK genes appear to play a pivotal role in the pathogenesis of NAFLD, a spectrum of liver disorders whose main clinical sign is insulin resistance due to impaired IRS signalling[67-68].

The role of different JNK genes in the process of hepatic steatosis exists significant conflict[69-70]. A much remarkable distinction between the JNK1 and JNK2 genes is the key role of JNK1 in the phosphorylation of the insulin receptor substrate-1 (IRS-1), associated with insulin resistance and obesity[71]. Moreover, acute knockdown of JNK1 or JNK2 in a model of established steatosis showed that the hepatocyte damage and steatosis were attenuated only in JNK1 knockdown not in JNK2 knockdown owing to increase expression levels of Bim[72]. Several other studies also have highlighted the importance of JNK1 over JNK2 in lung fibrosis, gastric cancer, histone acetylation, Bcl2 phosphorylation, repression of the Wnt/β-catenin signaling, and myoblast differentiation[73]. Therefore, these results stress the importance to better understand the individual and synergistic roles of JNK1 and JNK2 as pivotal mediators of obesity and insulin resistance in order to define potential therapeutic targets.

JNK is also involved in HSCs activation. Blocking JNK activity with small molecule drugs inhibited HSCs activation, shown by decreased expression of α-SMA, and reduced proliferation[74]. TGF-β, PDGF and angiotensin II up-regulate expression of α-SMA through activation of JNK. Both TGF-β and PDGF activate SMAD2 and

SMAD3 through JNK, resulting in HSC migration[59]. In addition, the role of different JNK genes is different for promoting HSC activation and proliferation. Jnk1$^{-/-}$ mice were protected from liver fibrosis, but Jnk2$^{-/-}$ mice showed significant fibrosis in cholestasis fibrosis model[59].

Together these data strongly suggest that JNK mediates many mechanisms that contribute to the pathogenesis of liver injury and more work is needed to better define the cell- and allele-specific role of JNK during liver fibrosis.

1.9 Aim of the study

Hepatic fibrosis is a wound-healing response to chronic liver injury, which frequently results in cirrhosis and consequently in liver failure. Chronic liver injury triggers a persistent and continuous response which increases ECM deposition. JNKs are activated in response to stimuli such as inflammatory cytokines, bacterial products, ROS, toxins, drugs, and metabolic changes. The JNK genes have been suggested to have a role during HSCs activation and differentiation which suggests a potential role for JNK in liver fibrosis. However, the specific role of the JNK genes, and specifically of JNK1, during liver fibrogenesis is not yet defined.

Therefore, in the present study we focused on the function and the cell-specific role of JNK1 in an animal model of chronic liver injury *in vivo*. We addressed this task by combining general and hepatocyte-specific JNK1 knockout animals ($Jnk1^{\Delta hepa}$). The different steps can be summarized as follows:

1. To study the contribution of JNK1 in hepatocytes and NPCs to chronic liver injury: Here, WT, $Jnk1^{-/-}$ and $Jnk1^{\Delta hepa}$ mice were subjected to either bile duct ligation (BDL) or CCl_4 for the induction of hepatic fibrosis. Thus, we analyzed whether JNK1 in hepatocytes or in NPCs has an impact on experimental liver fibrosis.

2. To analyse the function of JNK1 in BMCs during liver injury: To investigate whether BMCs are essential in promoting liver fibrosis, we performed BMT. WT and $Jnk1^{-/-}$ mice were lethally irradiated and reconstituted with either $Jnk1^{-/-}$ or WT BMCs. Five weeks later, recipient mice were subjected to chronic CCl_4 application or BDL surgery for 28 days.

3. To assess the role of JNK1 in HSCs *in vivo* and *in vitro*: Activated HSCs migrate and accumulate at the sites of tissue during chronic liver injury. Therefore, we tested the relevance of JNK1 during HSCs transdifferentiation into myofibroblasts. In these cells, proliferation, apoptosis and transdifferentiation were studied *in vitro* over a time period of 10 days.

2. Materials and Methods

2.1 Materials

2.1.1 Chemicals

Reagent	Manufacturer
Ac-DEVD-AFC Fluorogenic Substrate	Biomol, Hamburg
Acetic acid (glacial) 100% (CH_3COOH)	Merck, Darmstadt
Acetone (C_3H_6O)	VWR, Darmstadt
Acrylamide 30%	Bio-Rad, Munich
Agar-Agar	Becton Dickinson, Heidelberg
Agarose Electrophoresis Grade	Serva, Heidelberg
Albumin bovine	Sigma, Steinheim
Ammonium peroxodisulfat ($H_8N_2O_8S_2$)	Roth, Karlsruhe
Ampicilin	Sigma, Steinheim
Aprotinin	Sigma, Steinheim
Boric acid (H_3BO_3)	AppliChem, Darmstadt
Bromphenol blue	Bio-Rad, Munich
β-Mercaptoethanol	AppliChem, Darmstadt
CHAPS ($C_{32}H_{58}N_2O_7S$)	Sigma, Steinheim
Chloroform ($CHCl_3$)	AppliChem, Darmstadt
Collagen from rat tail	Sigma, Steinheim
Complete Mini (protease inhibitors)	Roche, Mannheim
Coomassie Brilliant Blue	Bio-Rad, Munich
DAKO REAL Peroxidase Blocking Solution	Dako, Hamburg
3,3 Diaminobenzidine tablets (Sigma fast)	Sigma, Steinheim
DMF (N,N-Dimethylformamid) $((CH_3)_2NC(O)H)$	Sigma, Steinheim
DMSO (Dimethyl sulfoxide)	Sigma, Steinheim
DNA standard	Invitrogen, Karsruhe
DTT (Dithiothreitol) ($C_4H_{10}O_2S_2$)	Sigma, Steinheim
EDTA (Ethylene Diamine Tetraacetate)	AppliChem, Darmstadt
EGTA (Ethylene glycol tetraacetic acid)	AppliChem, Darmstadt
Eosin	Sigma, Steinheim
Ethanol (C_2H_5OH)	AppliChem, Darmstadt
Ethidium bromide ($C_{21}H_{20}BrN_3$)	Invitrogen, Karsruhe
Fast Red Tablets	Roche, Mannheim
Fetal bovine serum	Invitrogen, Karsruhe
Formaldehyde 37% (CH_2O)	Roth, Karlsruhe
Gelatin from porcine skin Type A	Sigma, Steinheim

Glutaraldehyde ($C_5H_8O_2$)	Roth, Karlsruhe
Glycerin ($C_3H_5(OH)_3$)	Roth, Karlsruhe
Glycerol gelatin	Sigma, Steinheim
Glycine ($C_8H_9NO_3$)	AppliChem, Darmstadt
Goat serum	Promocell, Heidelberg
Haematoxylin	Sigma, Steinheim
HEPES ($C_8H_{18}N_2O_4S$)	Roth, Karlsruhe
Hydrogen peroxide 30% (H_2O_2)	AppliChem, Darmstadt
Hydrochloric acid (HCl)	Merck, Darmstadt
Isopropyl alcohol (C_3H_8O)	AppliChem, Darmstadt
Magnesium chloride ($MgCl_2$)	Merck, Darmstadt
Methanol (CH_4O)	VWR, Darmstadt
Nonfat dried milk powder	AppliChem, Darmstadt
Nonidet P-40	AppliChem, Darmstadt
Novex Sharp protein standard	Invitrogen, Karsruhe
Phenilenediamine dihydrochloride	Sigma, Steinheim
Paraformaldehyd ($(CH_2O)n$)	Roth, Karlsruhe
Pefabloc SC Protease Inhibitor	Roth, Karlsruhe
Penicillin-Streptomycin	Invitrogen, Karsruhe
peqGOLD RNA PureTM	Peqlab, Erlangen
PhosSTOP	Roche, Mannheim
PIPES ($C_8H_{18}N_2O_6S_2$)	Sigma, Steinheim
PMSF (Phenylmethylsulphonyl fluoride)	Roth, Karlsruhe
Poly dI:dC	GE Healthcare, Munich
Ponceau S	Sigma, Steinheim
Potassium chloride (KCl)	Merck, Darmstadt
Potassium Ferricyanide ($C_6N_6FeK_3$)	Sigma, Steinheim
Potassium Ferrocyanide ($C_6N_6FeK_4$)	Sigma, Steinheim
Roti-Histokit	Roth, Karlsruhe
SDS (Sodium Dodecylsulfate) ($NaC_{12}H_{25}SO_4$)	Roth, Karlsruhe
Serum, human	Sigma, Steinheim
Serum, mouse	Sigma, Steinheim
Serum, rabbit	Sigma, Steinheim
Sodium acetate anhydrous ($C_2H_3NaO_2$)	AppliChem, Darmstadt
Sodium azide (NaN_3)	AppliChem, Darmstadt
Sodium tetraborate anhydrous ($Na_2B_4O_7$)	Sigma, Steinheim
Sodium carbonate (Na_2CO_3)	Merck, Darmstadt
Sodium chloride (NaCl)	AppliChem, Darmstadt
Sodium fluoride (NaF)	Sigma, Steinheim

Sodium hydroxide (NaOH) 1 mol/l	AppliChem, Darmstadt
Sodium hydroxide pellets	Merck, Darmstadt
Sodium orthovanadate (Na_3VO_4)	AppliChem, Darmstadt
Sodium thiosulfate ($Na_2S_2O_3$)	Sigma, Steinheim
SuperSignal West Pico Substrate	Thermo Scientific, Bonn
TEMED (Tetramethylethylenediamine)	Bio-Rad, Munich
Tissue Tek	Dako, Hamburg
Trichloroacetic acid ($C_2HCl_3O_2$)	Merck, Darmstadt
Trypsin Inhibitor	Sigma, Steinheim
Tris ($C_4H_{11}NO_3$)	AppliChem, Darmstadt
Tri-sodium citrate dihydrate ($Na_3C_6H_5O_7 \cdot 2HCl$)	Roth, Karlsruhe
Triton X100	Roth, Karlsruhe
Trypton	Becton Dickinson, Heidelberg
Tween® 20	Sigma, Steinheim
Vectashield mounting medium with DAPI	Dako, Hamburg
Vectastain ABC Kit	Dako, Hamburg
Xylene	VWR, Darmstadt

2.1.2 Standard buffer and media

Buffers	**Manufacturer**
Phosphate buffered saline (PBS)	PAA, Cölbe
Restore Western Blot Stripping Buffer	Thermo Scientific, Bonn
Roti Block 10x	Roth, Karlsruhe
Rothiphorese10x SDS PAGE	Roth, Karlsruhe
TAE 50x	AppliChem, Darmstadt

Cell culture medium	**Manufacturer**
DMEM (Dulbeco's Modified Eagle Medium)	PAA, Cölbe
EBSS (Earle's Balanced Salt Solution) w/o Ca^{2+} & Mg^{2+}	Invitrogen, Karsruhe
EBSS (Earle's Balanced Salt Solution) with Ca^{2+} & Mg^{2+}	Invitrogen, Karsruhe
HBSS (Hank's Balanced Salt Solution)	PAA, Cölbe
RPMI (Roswell Park Memorial Institute)	PAA, Cölbe

2.1.3 Standard kits and enzymes

Kit / Assay	Manufacturer
BIO-RAD Protein Assay	Bio-Rad, Munich
In Situ Cell Death Detection Kit, Fluorescein	Roche, Mannheim
Omniscript RT Kit	Qiagen, Hilden
OxiSelect Oxidative DNA Damage Quatitation Kit (AP sites)	Cell Biolabs / Biocat, Heidelberg

Enzyme	Manufacturer
Collagenase Type II	CellSystems, Troisdorf
HotStarTaqTM Master Mix	Qiagen, Hilden
Proteinase K – Solution	AppliChem, Darmstadt
ReadyMixTM redtaqTM PCR reaction mix with $MgCl_2$	Sigma, Steinheim
RNAse	Sigma, Steinheim
SYBR® GreenERTM qPCR Super Mix	Invitrogen, Karlsruhe

2.1.4 Antibodies used for immunostaining and/or western blot

Primary Antibody	Catalog Number	Company
α-SMA	A2574	Sigma
CD11b	550282	BD
Cleaved caspase-3	#9661	Cell Signaling
CK19	12-3900	Santa Cruz
CollagenI α1	BT-5014-10	BioTrend
Cyclin A	sc-596	Santa Cruz
Cyclin D	sc-450	Santa Cruz
F4/80	MCA497GA	AbD serotec
Ki-67	6013874	Leica
PCNA	13-3900	Invitrogen
JNK1	3708s	Cell Signaling
JNK2	4672s	Cell Signaling
JNK	9252s	Cell Signaling
pJNK1/2	9251	Cell Signaling

Secondary Antibody	Catalog Number	Company
Anti-rabbit HRP	#7074	Cell Signaling
Anti-mouse HRP	sc-2954	Santa Cruz
Anti-goat HRP	sc-2768	Santa Cruz
Anti-rat HRP	sc-2956	Santa Cruz
Alexa Fluor488 anti-mouse	A-11059	Invitrogen
Alexa Fluor 488 anti-rabbit	A-11008	Invitrogen
Alexa Fluor 546 anti-rabbit	A-11071	Invitrogen
Alexa Fluor 594 anti-rabbit	A-11072	Invitrogen

2.1.5 Primer sequences used for qRT-PCR

Gene	Forward	Reverse
α-SMA	ATG AAG CCC AGA GCA AGA GA	ATG TCG TCC AGT TGG TGA T
Collagen1α	GGA AAC CTC TCT CGC CTC TT	GAA CAG GGT GTT CCT GAG A
CK19	CGT ACC CCC AAA GGA AGA CA	TCA GAC CTG CGT CCC TTT TT
CcnA2	GTG GTG ATT CAA AAC TGC CA	AGAGTGTGAAGATGCCCTGG
CcnD1	AAG CAT GCA CAG ACC TTT GTG G	TTCAGGCCTTGCATCGCAGC
CcnE1	TCC ACG CAT GCT GAA TTA TC	TTGCAAGACCCAGATGAAGA
GAPDH	TGT TGA AGT CAC AGG AGA CAA CCT	AAC CTG CCA AGT ATG ATG ACA TCA
IL-1α	TGG GAG CCC TTT CAT CAT GAT	AAG GAC GGG AGG GAG AAA GAC T
IL-6	CTT CCA TCC AGT TGC CTT CTT	AAT TAA GCC TCC GAC TTG TGA AG
MMP2	GGC AAT GCA GAT GGA CAG CC	CAT AGT CCT CGG TGG TGC C
TGF-β1	AAA AAC CAA AGC CCA AAA AGC TA	ATG ACT CAC ACT GAC GCA GAA AA
TIMP1	GGT CCG AGT TGC AGA AGG C	GGC ATC TGG CAT CCT CTT G
TNF-α	CAT TCG AGG CTC CAG TGA ATT C	GAA ACA CAA GAT GCT GGG ACA GT

2.1.6 Primer sequences used for genotyping PCR

Mouse strain	Primer name	sequence
JNK1	fw	CAC ATA CAC TCA GTG GAT CT
	re	CAC TAT TGC CTT AAG ACT CC
	fm	CTG ATC TTC CAG ATA ACT GC
JNK2	fw	TCC AGT ACA GCG CGG CTG AA
	re	GCA GCA GCC CTC AGG ATC CT
	fm	TCT GAC GTC CTG GGC TGG AC
pAlb-cre	fw	CGG GTG AAC GTG CAA AAC AGG CTC
	re	CTT GCA TGA CCG GTA TTG AAA CTC CAG
JNK1$^{\Delta hepa}$	fw	GAA CCA CTG TTC CAA TTT CCA TCC
	re	GGA TTT ATG CCC TCT GCT TGT C

2.1.7 Instruments and other equipment

Instrument	Manufacturer
AxioImager Z1	Carl Zeiss, Jena
Blotting chamber Trans-Blot cell	Biorad, Munich
Bright Field Microscope DM1000	Leica, Wetzlar
Cell culture bench BSB6A	Gelaire Flow Laboratories, Meckenheim
Cell incubator Haereus BB 6220	Thermo Scientific, Dreieich
Centrifuge Eppendorf Tabletop 5417	Eppendorf, Hamburg
Centrifuge Heraeus-Kendro Megafuge 1.0R	Thermo Scientific, Dreieich
Centrifuge Heraeus Pico 17	Thermo Scientific, Dreieich
Cryostat HM 550	Microm Thermo Scientific, Dreieich
DISKUS Z16 APO	Leica, Wetzlar
FACS Canto II Flow Cytometer	BD, Erlangen
FUJI FILM LAS-4000	FUJI FILM Europe, Düsseldorf
Gel chamber Subcell GT	Biorad, München
Gel chamber	Peqlab, Erlangen
Homogenizer	Janke & Kunkel, Staufen
Microcentrifuge IR 220 VAC	Roth, Karlsruhe
Real-Time PCR System 7300	Applied Biosystems, Darmstadt
Thermocycler T3000	Biometra, Göttingen
Thermomixer	Eppendorf, Hamburg
Vortex Reax top	Heidolph, Nürnberg

Animal experiment consumables	**Manufacturer**
General chow for rodents	Altromin, Lage
Hematocrit capillary	Hirschmann Laborgeräte, Eberstadt
Heparine (Liquemin(R))	Roche, Mannheim
Injection needles Sterican(R)	Braun, Melsungen
Isoflurane	Abbott, Ludwigshafen
Ketamin 10%	CEVA TIERGESUNDHEIT GmbH, Düsseldorf
Micro tube (1,1 ml Z-Gel)	Sarstedt, Nümbrecht
Sodium chloride 0,9% (NaCl)	DeltaSelect, Dreieich
Sunflower seed oil	Sigma, Steinheim
Surgical instruments	FST, Heidelberg
Syringe Omnican(R)	Braun, Melsungen
Xylazin 2%	Bernburg Medistar, Holzwickede

Plastic and Glassware	**Manufacturer**
Beakers (10 – 1000 mL)	Schott-Duran, Mainz
Bottles (25- 2000 mL)	Schott-Duran, Mainz
SuperFrost slides	Roth, Karlsruhe
Pasteur pipettes	Brand, Giessen
96-well plates for RNA/DNA measurement	Greiner Bio-one, Frickenhausen
96-well plates for protein measurement	Greiner Bio-one, Frickenhausen
96-well plates for Real-Time PCR	StarLab, Ahrensburg
Pipettes tips with filter for liquid handling	VWR, Darmstadt; BioHit, Rosbach v.d. Höhe; Biozym, Hess. Oldendorf
Reaction tubes (0,5 – 2mL)	Eppendorf, Hamburg
8 vial strips for PCR (0,2mL)	Sarstedt, Nümbrecht
Reaction tubes 15mL	Sarstedt, Nümbrecht
Reaction tubes 50 mL	GreinerBio-one, Frickenhausen
Sterile pipettes (2-50mL)	Sarstedt, Nümbrecht
Cell Strainer (70 µm)	BD, Erlangen
Cryotubes 1,5 mL	Nunc, Langenselbold
6; 12; 24-well plates	BD-Falcon, Heidelberg

2.2 Methods

2.2.1 Bile duct ligation

8-10 weeks-old mice were narcotized using 0.01% Xylazin hydrochloride/ 1% Ketamin hydrochloride mixture, diluted in 0.9% NaCl. Per each 10 g body weight of the mouse, 100 µl of the narcotization-solution was administrated. After reflex control and affirmation of narcotization, the abdominal wall was sterilized by using Antifect®. Afterwards, an abdominal midline skin incision is made through the abdominal musculature by 1.5 cm long cut. The lobes of the liver are gently retracted to expose the bile duct. The bile duct then is carefully ligated with two pieces of sutures that one is in dorsal and the other is ventral to the bile duct. A small incision is used between both ligatures to ensure blocking of the bile duct. The abdominal musculature and skin are closed with absorbable suture by a continuous fissure. Subsequently, mice were received 150 µg Temgesic® i.p. to avoid pain-induced stress.

2.2.2 Bone marrow transplantation

a) Treatment of donor mice: BMCs are isolated from euthanized donor mice. The concentration of cells is 10^7 cells /ml and each lethally irradiated mouse will receive a single intravenous (tail vein) or retro-orbital injection of donor BMC (1×10^6) cells.

b) Treatment of recipient mice: Irradiation of recipient mice is performed by using a cobalt irradiator in one of the barrier facilities. Mice are placed into a rotating pie-shaped holder (to limit mobility and insure equal irradiation), which is then secured in the irradiator to deliver a dose of 6.8 G. The mice will be in the irradiator 8 minutes. Irradiation is repeated 4 h later for a total dose of 13.6 G (split dose irradiation is used to limit the non-hematopoietic toxicity - usually intestinal damage). Irradiated mice are injected within 18 h after the second irradiation via the tail vein with donor BMCs (1×10^6) diluted in 100 µl of sterile PBS. Alternatively, the cells may be

injected retro-orbitally into anesthetized mice. Recipient mice are maintained on antibiotic-containing water for approximately 2 weeks.

2.2.3 Isolation of HSCs with FACS Sorting

All cells were prepared from adult male C57BL/6 mice weighting approximately 35 g, with free access to a standard chow diet and water. HSCs were isolated following the collagenase method, adapted to the murine system. Two animals each were taken for individual cell preparations. They were anesthetized with an intramuscular injection of Ketamin and Xylazin, and livers perfused via the portal vein with pronase and collagenase. The liver capsules were removed, tissues homogenized and further digested in a solution containing DNase I. The resulting cell suspensions were filtered through a nylon mesh, centrifuged and washed in ice cold Hanks buffered standard saline (HBSS; PAA Laboratories GmbH, Linz, Austria) containing 0.25% (w/v) BSA. HSCs were further purified by a single-step density gradient centrifugation with 8.2% (w/v) Nycodenz (Axis-Shield Point-of-Care Division, Oslo, Norway). HSCs were collected by aspiration of the white top layer of the gradient.

After this step our team have established protocols to isolate HSCs by FACS[5]. HSCs from rats were purified by cell sorting using simply their high side scatter of incident light. Starting from crude cell fractions that were 50–70% enriched by conventional density centrifugation, the obtained cell purity after sorting (in which 1.4 ± 0.4 million cells were sorted per hour) was found to be over 96% and the viability of resulting cells was approximately 90%, as measured by Trypan blue exclusion testing. Freshly isolated HSCs were washed and plated in 6-well plates (Falcon) at a density of 150.000 cells per well and cultivated in DMEM supplemented with 10% FCS 4 mmol/l L-Glutamine and 4 mmol/l Penecillin/Streptomycin (PAA, Pasching, Austria). After 6-8 h cells were attached and medium was changed. At indicated time points (day 1, 4, 7, 10 after isolation, respectively), cells were harvested with Accutase© (eBioscience, Frankfurt, Germany), washed with phosphate buffered saline and fixed with 4% PFA for 25 min. After fixation cells were stained as required.

2.2.4 Microarray analysis

RNA was isolated from mouse livers using TRIzol reagent and purified with the RNeasy Mini Kit (Qiagen, Venlo, The Netherlands) according to the manufacturer's instructions. Concentrations and purity of RNA samples were determined on a NanoDrop ND-1000 spectrophotometer (Isogen, Maarssen, Netherlands). RNA integrity was checked on an Agilent 2100 bioanalyzer (Agilent Technologies, Amsterdam, The Netherlands) with 6000 Nano Chips. RNA samples from 3 mice per experimental group were used for microarray analysis. Samples were hybridized on Affymetrix GeneChip Mouse Genome 430 2.0 arrays in the microarray core laboratory of the Nutrigenomics Consortium at Wageningen University, The Netherlands. Hybridization, washing, and scanning of the arrays were performed according to standard Affymetrix protocols. Array images were processed using packages from the Bioconductor project[75]. Probe sets were redefined according to Dai[76]. Probes were assigned to unique gene identifiers, in this case Entrez IDs. Arrays were normalized with the Robust Multi-array Average (RMA) method. Differentially expressed probe sets were identified using intensity-based moderated paired t-statistics. P values were corrected for multiple testing using a false discovery rate (FDR) method.

2.2.5 Housing and breeding of mice

Animal husbandry and procedures were approved by the authority for environment conservation and consumer protection of the state North Rhine–Westfalia (LANUV, Germany) and the University Hospital RWTH Aachen Animal Care Facility's guidelines. For our study we used mice of male gender with constitutive deletion of $Jnk1^{-/-}$ and $Jnk1^{\Delta hepa}$ mice and WT littermates from heterozygous breeding couples.

2.2.6 Induction of liver fibrosis in mice

Experiments were performed with age-matched male mice at the age of 7 to 8 weeks. Mice were treated with CCl_4, (Merck; 0.6 mL/kg of body weight) diluted in

corn oil and BDL. Control animals were treated with corn oil only and sham. To induce CCl_4 mediated chronic liver injury, mice (n=9-10 per group) received a single i.p. injection of CCl_4 and were sacrificed 72 h after the last injection. The same number of mice were performed by BDL and sacrificed after 4 weeks.

2.2.7 Genotyping

The correct genotypes were verified by PCR analysis. DNA was prepared from fresh mouse tail biopsies using NID buffer. Mouse tails were digested with 200 µl of NID buffer and 1 µl of proteinase K at 56°C overnight. Enzyme activity was stopped by heating at 95°C for 5 minutes. The tairs were shortly spun down and 2 µl of the supernatant was used for PCR reaction.

NID buffer content	End concentration
KCl	0.05 M
Tris	0.01 M
$MgCl_2$	2 mM
Gelatine type 3	0.1 mg/ml
NP-40	0.45 %
Tween 20	0.45 %

PCR reaction and programs were as follows:

Reaction volume	25 µl
Primer sense (0,1nmol)	1 µl
Primer antisense (0,1nmol)	1 µl
Polymerase mix *	12.5 µl
dH_2O	8.5 µl
DNA template	2 µl

* ReadyMixTM redtaqTM or HotStarTaqTM Master Mix

PCR products were separated by size on 2% (w/v) agarose gels. The agarose was boiled in TAE buffer, cooled at RT for 5-10 min, and 0.4 µg/ml ethidium bromide (EtBr) was added. 5x loading dye were added to the samples before application to the gel slots. Gels were run in TAE at 100-150 V. DNA markers were used to determine the specific size of fragments. EtBr, which intercalates into the DNA, enables the visualisation of the DNA on a UV-transilluminator.

2.2.8 Blood sampling and serology

Blood sampling was performed in mice under transient anesthesia with isoflurane by penetrating the retro-orbital sinus with a glass capillary. Blood samples were collected in a serum tube and centrifuged at 5000 *g* for 10 minutes. Serum was transferred into a fresh tube and stored at -20°C. Serum transaminases are specific markers for liver damage. For this study, ALT and AST were measured in the clinical laboratories of the Institute of Clinical Chemistry and Pathobiochemistry, UK Aachen.

2.2.9 Liver perfusion and isolation of primary hepatocytes

The mice were anaesthetized by intraperitoneal injection of ~300 µl of Ketamin-Xylazin solution. Anesthetized mice were immobilized with tape on all four limbs, the abdomen was opened and intestine was moved aside to expose the portal vein. The cannula was inserted in the portal vein and was fixed with a nylon monofilament wire to avoid that the blood pressure removes the needle at the beginning of the perfusion. Perfusion was started with 30 ml solution A, pH 7.4. As soon as the perfusion is started, the hepatic vein was immediately cut to allow perfusate to run out. Liver was perfused with a flow rate of 5 ml/min. Next, the liver was perfused with 30 ml of B solution pH 7.4. Finally, perfusing was switched to solution C with collagenase. At this stage the hepatic tissue was rapidly disaggregated. The tissue was collected and transferred into a plate, gallbladder was removed, and the liver tissue is swirled around to wash hepatocytes out.

Perfusion solutions	Content	Amount
Solution A	EBSS without Ca^{2+} & Mg^{2+}	50 ml
	EGTA	100 mM
Solution B	EBSS with Ca^{2+} & Mg^{2+}	30 ml
	HEPES, pH 7.4	10 mM
Solution C	EBSS with Ca^{2+} & Mg^{2+}	50 ml
	HEPES, pH 7.4	10 mM
	Collagenase	0.3 mg/ml
	Soybean trypsin inhibitor	0.04 mg/ml

Hepatocytes and remaining tissue were collected in 5 ml DMEM and filtered through a 70 µm cell strainer. Cells were centrifuged at 500rpm for 1min at room temperature. Pellet was washed with PBS twice. Supernatant was removed and the pellet was resuspended in 20 ml high glucose DMEM supplemented with serum (10% FCS) and antibiotics (Penicillin, Streptomycin). The hepatocytes were counted and plated on precoated plates (Collagen from mouse tail). Mouse primary hepatocytes were cultured in DMEM/high glucose media supplemented with 10% FCS in a humidified atmosphere containing 5% CO_2 at 37°C. The cells were grown in 100 mm dishes, 6-well or 96-well plates. The cells were allowed to settle down and adhere to culture dishes for 4-5 h and then the medium was replaced with fresh one or immediately stimulated.

2.2.10 RNA extraction, cDNA preparation, Real-Time PCR

RNA was extracted from mouse livers or primary hepatocytes using peqGOLD RNA PureTM (Peqlab) following manufacturer's instructions. A piece of liver tissue was minced in peqGOLD RNA with an electric homogenizer. Lysates were incubated at RT for five minutes. After addition of 0.2 volumes of chloroform to the supernatants followed by centrifugation at 12000 *g*, the upper phases were incubated 10 minutes with isopropanol and RNA was pelleted by centrifugation at 12000 *g* at 4°C. The pellets were washed tiwce with 1 ml of 70% ethanol, air dried for 5 minutes and eluted in RNAse-free water. RNAs were quantified by spectrophotometry at an optical density (OD) of 260 nm. A 260/280 ratio ≤2.0 and ≥1.8 was considered high purity.

Reverse transcription reaction mix	**Volume per reaction**
10x Buffer RT	2 µl
dNTP mix	2 µl
Oligo DT	2 µl
Omniscript Reverse transcriptase	1 µl
Template RNA (1µg/µl)	2 µl
Total reaction volume	**20 µl**

Reverse transcription was performed using an Omniscript kit (Qiagen) according to the manufacturer's protocol. Reactions were carried out in 20 µl volumes. Reactions were incubated in a PCR thermocycler at 37°C for 60 min, and 95°C for 5 min and then cooled to 4°C. After reverse transcriptase, samples were diluted by adding purified water.

For real-time quantitative RT-PCR, the Real-Time PCR System (AB 7300) was used. RT-PCR was performed in duplicate in 25 µl reaction volumes. Three-step PCR cycling was carried out as follows: 50 °C for 2 min (1 cycle), 95°C for 10 min (1 cycle), 95°C for 15 s, and 60°C for 1 min (40 cycles). At the end of the PCR, baselines and threshold values were established using AB 7300 System SDS software, and the Ct values were exported to Microsoft Excel for analysis. Expression of mRNA was calculated using a relative quantification method [77], which determines the relative quantification of a target gene in comparison to a control gene. Analysis was carried out using the sequence detection software. This software calculates the Ct for each reaction and uses it to quantify the amount of starting template in the reaction. The relative expression ratio of a target gene is calculated based Ct deviation of an unknown sample versus a control and is expressed in comparison to the reference gene GAPDH.

Real-time PCR reaction mix	**Volume per reaction**
Primer sense	2 µl
Primer antisense	2 µl
SYBR green	12.5 µl
cDNA	5 µl
dH_2O	3.5 µl
Total reaction volume	**25 µl**

2.2.11 Protein concentration measurement

The concentration of whole protein extracts was performed using BIO-RAD Protein Assay reagent. This technique was first described by Bradford *et al*[78] and based on the absorbance maximum for an acidic solution of Coomassie Brilliant Blue G-250 shifts from 465 nm to 595 nm when binding to protein occurs. According to manufacturer's protocol protein and standard were measured in a spectrophotometer

at OD595. The OD595 of each sample was compared to a standard curve prepared with BSA.

2.2.12 Western Blot

Protein samples were separated electrophoretically on 10%, 12% or 15% denaturing SDS-polyacrylamide gel or on pre-cast 4-12% polyacrylamide gel (Invitrogen). Gel and buffer were prepared according to table (see below).

In short, 6 times protein loading buffer was added to each sample in appropriate volumes and samples were boiled at 96 °C for 5 min before loading to the gel slot. Separation was performed in 1x SDS running buffer at 80 V overnight or in MOPS running buffer at 120 V for approximately 2 h (pre-cast gel system). For immunological detection, the separated proteins in gel were transferred to a nitrocellulose membrane.

Reagent	**Resolving Gel**		
Percent	**15%**	**10%**	**12.5%**
dH_2O	12.3 ml	20 ml	16.4 ml
1.5M Tris-HCl, pH 8.8	12.5 ml	12.5 ml	12.5 ml
0.5M Tris-HCl, pH 6.8	-	-	-
30% Acrylamide	24.35 ml	16.5 ml	20.3 ml
10 % SDS	500 µl	500 µl	500 µl
10 % APS	500 µl	500 µl	500 µl

A wet blotting chamber was used to transfer the separated proteins from the polyacrylamide gel to a nitrocellulose membrane. Whatman paper, nitrocellulose membrane and polyacrylamide gel were soaked in transfer buffer. Transfer was performed according to standard proceedings.

Successful transfer was confirmed by Ponceau Red staining. For immunological detections, the non-specific binding sites were blocked for 1 hours in 2.5% non-fat dry milk diluted in PBS-Tween (PBST) or in 1x Roti-block. The membrane was shortly washed and then incubated overnight at 4°C in PBST with primary antibody at optimized dilutions. The membrane was washed 3x10 min in PBST and then incubated with the secondary antibody diluted 1:2000 in PBST for 1h

at RT. After incubation, the membrane was washed 3x5 min in PBST and then incubated in ECL Substrate (Pierce) for 5 min. The membrane was exposed to hyperfilm (Amersham) or a digital detection system.

2.2.13 Immunofluorescence staining

Cryopreserved sections were dryed in air 7 minutes. Sections (5 µm), from mouse livers, were fixed with 4% PFA for 15 min and washed with PBS for 3 x 5 min. All subsequent steps were carried out at RT in the humidified chamber. PBS containing 5% goat serum and 0.3% Triton was used for blocking for one hour followed by an overnight incubation with primary antibody in blocking solution at optimized dilutions at 4°C. Slides were washed with PBS for 3 x 5 min and incubated with secondary antibody labelled with Alexa fluorescent dye in blocking buffer for one hour at RT. Slides were washed with PBS for 3 x 5 min. Nuclei were counterstained with DAPI in mounting medium.

TUNEL (TdT-mediated dUTP nick end labelling) staining is an established method for in situ labelling of DNA strand brakes that occur early during apoptosis. Terminal deoxynucleotidyl transferase (TdT) is used to introduce labelled nucleotides into partially degraded DNA. Liver cryosections were fixed with 4% PFA for 45 min and rehydrated with PBS for 3 x 10 min. Sections were treated with 3% H_2O_2 in methanol for 10 min, and then permeabilized with 0.1% Triton 100x, 0.1% Na-citrate for 2 min at 4°C. Slides were washed with PBS and stained with TUNEL mix (1µl enzyme, 9 µl TUNEL dilution buffer, 90 µl buffer) in humidified chamber overnight at 4°C. After 3 x 10 min washing with PBS stained sections were mounted with DAPI mounting medium. The percentage of TUNEL positive cells was counted and set in percentage relationship to TUNEL negative.

2.2.14 Immunohistochemistry

Paraffin embedded sections were dewaxed and rehydrated with xylene and decreasing percentages of ethanol. Antigen retrieval was performed by cooking sections in sodium citrate buffer for 6 minutes in a microwave (Do not let the slides

go dry). This step enhances the availability of the antigen. After cooling for 10 minutes, sections were rinsed in running tap water and endogenous peroxidases were quenched for 10 minutes. Sections were washed under running water, washed 2 x 5 minutes in PBS. Following blocking with Avidein D blocking reagent for 15 minutes at RT and with Biotin blocking reagent for 15 minutes at RT, sections were blocked in PBT (PBS, 0.1% BSA, 0.2% TritonX-100) and then incubated overnight with primary antibody (1:1000) at 4°C in a humid atmosphere. Slides were washed twice with PBS and the secondary antibody (1:200) was applied for 1 hour at RT in humidifying box, the parallel the HRP-ABC solution was made and incubated at least 30 minutes at RT prior to use. Sections were incubated with HRP-ABC solution for 1 hour at RT in a humidified box. After washing twice in PBS, signal was developed with DAB and counterstained with hematoxylin. Dehydrating was performed increasing percentages of ethanol and xylene, mounted with Roti-histokit.

2.2.15 Statistical analysis

All data are expressed as mean ± standard deviation of the mean. Statistical significance was determined by two-way analysis of variance followed by a Student's t test or by one-way ANOVA of GraphPad software. P values less than 0.05 were considered significant.

3. RESULTS

3.1 JNK1 in hepatocytes has no impact on hepatic injury during experimental liver fibrosis.

To investigate the relevance of hepatocyte-specific JNK1 expression for liver injury, we generated hepatocyte-specific JNK1 knockout mice ($Jnk1^{\Delta hepa}$). Besides $Jnk1^{\Delta hepa}$ animals constitutive $Jnk1^{-/-}$ and respective WT controls (floxed mice) were included in this analysis. Primary hepatocytes from the different animal strains were isolated and JNK1 protein expression was studied. These results confirmed lack of JNK1 expression in primary hepatocytes derived from $Jnk1^{-/-}$ and $Jnk1^{\Delta hepa}$ in contrast to WT mice (Figure 4A). Additionally, PCR of tail DNA confirmed the correct genomic changes in the JNK1 gene for the respective knockout strain (Figure 4B).

A B

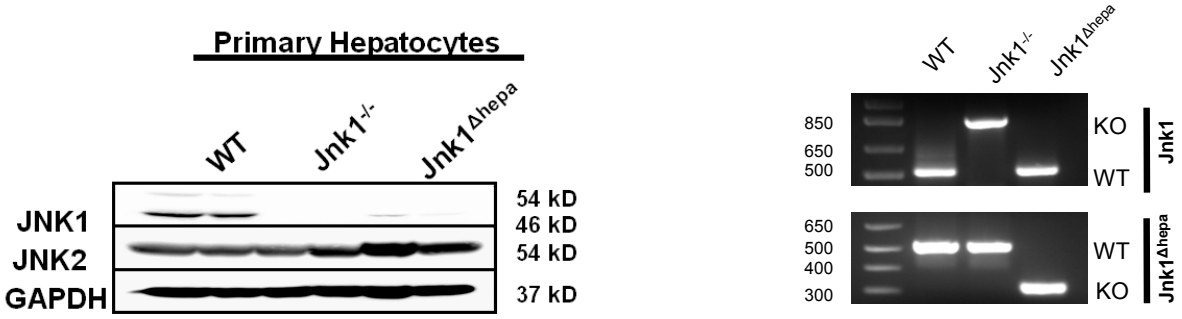

Figure 4. Lack of JNK1 expression in primary hepatocytes derived from $Jnk1^{-/-}$ and $Jnk1^{\Delta hepa}$ mice. (A) Primary hepatocytes of WT, $Jnk1^{-/-}$ and $Jnk1^{\Delta hepa}$ mice were examined by Western blot analysis by probing with antibodies to JNK1, JNK2 and GAPDH as indicated. **(B)** Ethidium Bromide gel showing the respective PCR results from tail DNA prepared from WT, $Jnk1^{-/-}$ and $Jnk1^{\Delta hepa}$ mice. The upper gel shows the detection of the WT and the constitutive JNK1 knockout locus, while the lower gel shows the WT and the floxed JNK1 gene locus.

WT, $Jnk1^{-/-}$ and $Jnk1^{\Delta hepa}$ were treated with CCl_4 or with BDL for 4 weeks. Macroscopic analysis of livers from CCl_4-treated mice showed no apparent difference compared with corn oil-injected controls (Figure 5A). However, H&E staining of $Jnk1^{\Delta hepa}$ and WT livers treated for 4 weeks with CCl_4 revealed more cellular damage and centrilobular congestion of inflammatory cells compared to $Jnk1^{-/-}$ mice (Figure 5B).

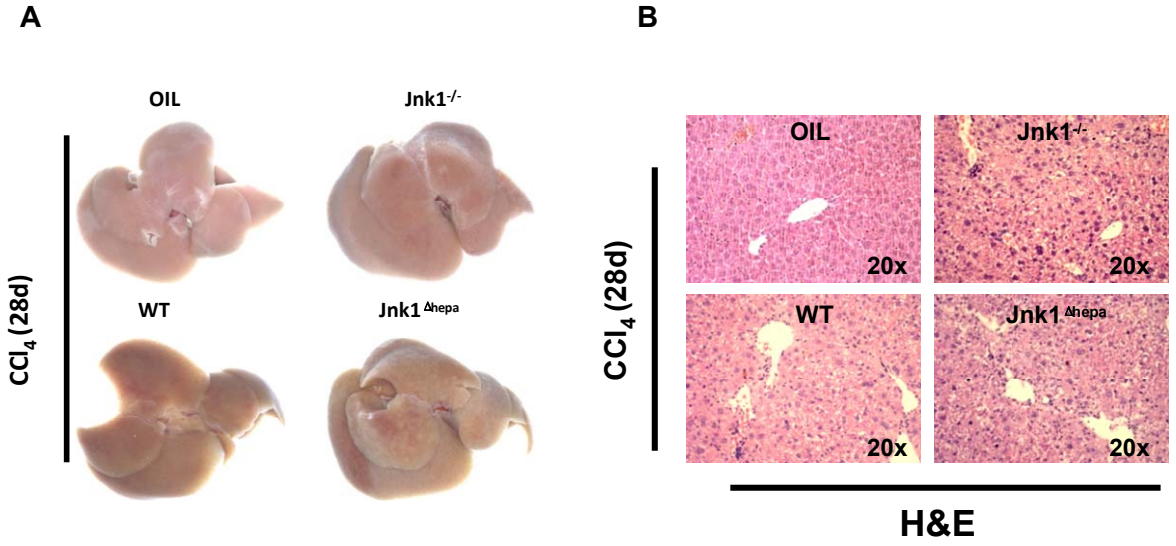

Figure 5. Macroscopic appearance and H&E staining of livers from CCl_4-treated mice. (A) Macroscopic appearance of livers of WT, Jnk1$^{-/-}$ and Jnk1$^{\Delta hepa}$ mice 28 days after repeated CCl_4 njections. Corn-oil injections were used as controls. **(B)** Representative H&E staining of liver sections from livers of WT, Jnk1$^{-/-}$ and Jnk1$^{\Delta hepa}$ mice 28 days after repeated CCl_4 injections. Corn-oil injections were used as controls.

Macroscopic examination of 28 days-BDL-subjected liver specimens of WT and Jnk1$^{\Delta hepa}$ mice revealed the presence of necrotic foci in distinct hepatic lobes with yellowish color (Figure 6A). H&E staining of WT and Jnk1$^{\Delta hepa}$ livers showed severe cholestatic hepatitis with widespread bile infarcts - coincident with necrotic foci - along with bile ductular proliferation, portal edema and hepatocellular damage (Figure 6B+C). In contrast, Jnk1$^{-/-}$ mice exhibited signs of ductular proliferation but no necrotic foci (Figure 6B+C). Biliary infarcts in Jnk1$^{-/-}$ mice compared with WT and Jnk1$^{\Delta hepa}$ 4 weeks after BDL were dramatically reduced (Figure 6D). These data indicate that JNK1 expression in hepatocytes has no impact on hepatocellular injury in two different models of chronic experimental liver injury.

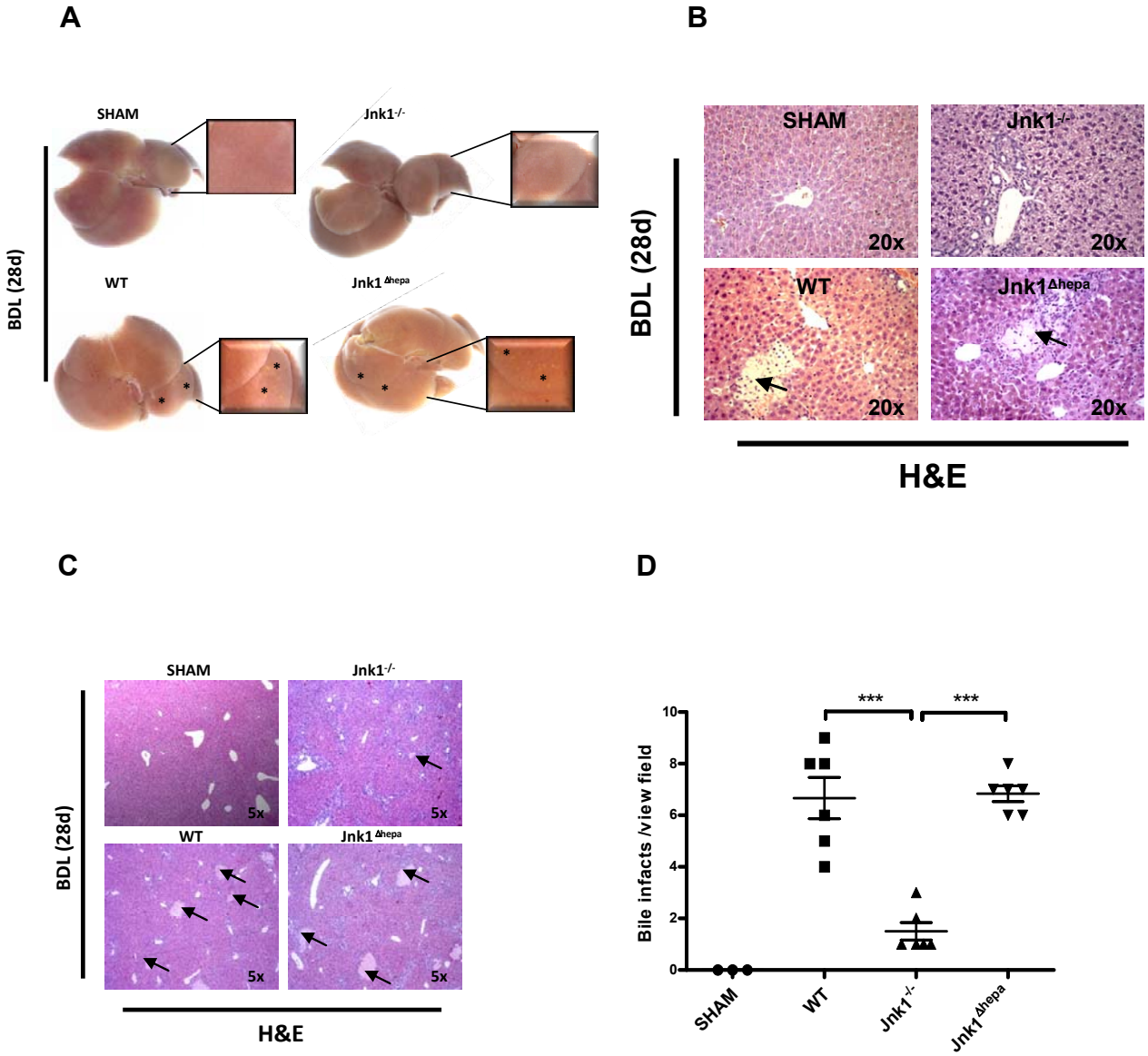

Figure 6. Presence of necrotic foci and biliary infarcts in BDL-subjected liver specimens. (A) Macroscopic appearance of livers of WT, Jnk1$^{-/-}$ and Jnk1$^{\Delta hepa}$ mice 28 days after BDL with detail of the liver surface. Sham-operated mice were used as controls. (*) indicate yellow dots on liver surface. **(B)** Representative H&E staining of liver sections from livers of WT, Jnk1$^{-/-}$ and Jnk1$^{\Delta hepa}$ mice 28 days after BDL. Sham mice were used as controls. Arrows (↑) indicate necrotic foci. **(C)** Representative H&E staining of livers of WT, Jnk1$^{-/-}$ and Jnk1$^{\Delta hepa}$ mice showing areas of necrotic foci (*). **(D)** Quantification of bile infarcts of WT, Jnk1$^{-/-}$ and Jnk1$^{\Delta hepa}$ mice 28 days after BDL was performed by a pathologist (Prof. N. Gaßler, Institute of Pathology, UKA).

As BDL triggers liver damage through biliary fibrosis, we analyzed biochemical markers 28 days after BDL. Plasma AST and ALT levels increased approximately 10-fold in Jnk1$^{\Delta hepa}$ and WT but only 7-fold in Jnk1$^{-/-}$ mice compared with respective sham-operated animals (Figure 7A+B). Bile duct ligated Jnk1$^{\Delta hepa}$ and WT mice

exhibited significantly more cholestasis as characterized by hyperbilirubinemia with yellowish skin and alkaline phosphatase (AP) compared with Jnk1$^{-/-}$ mice (Figure 7C+D).

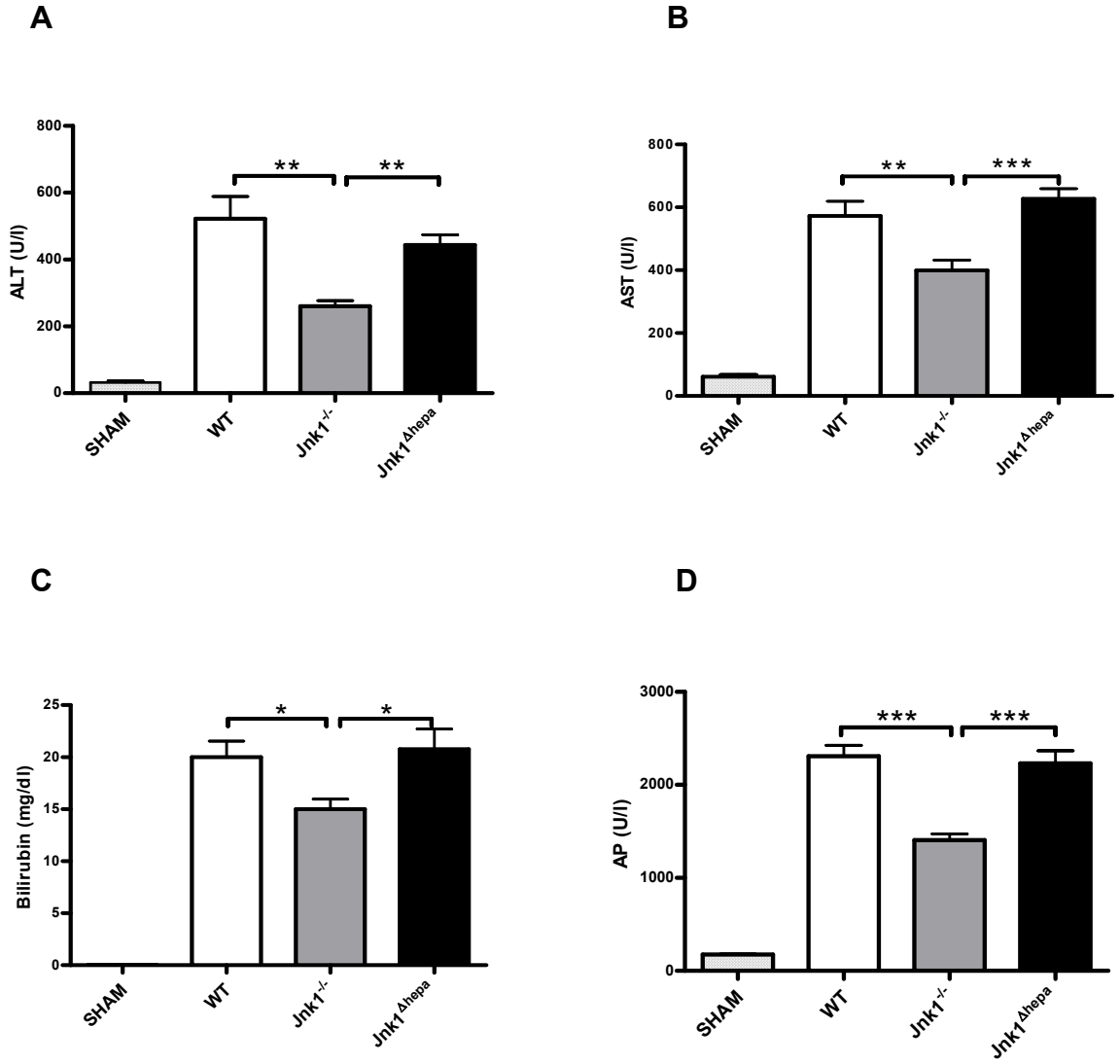

Figure 7. Biochemical markers of 28 days-BDL-subjected serum specimens. (A) Serum levels of AST were determined 28 days after BDL in SHAM, WT, Jnk1$^{-/-}$ Jnk1$^{\Delta hepa}$ mice.**(B)** ALT, **(C)** Bilirubin and **(D)** AP were determined 28 days after BDL in SHAM,WT, Jnk1$^{-/-}$ Jnk1$^{\Delta hepa}$ mice.

Death of hepatic cells was examined by TUNEL staining. Jnk1$^{-/-}$ animals showed significantly less TUNEL-positive cells than WT and Jnk1$^{\Delta hepa}$ mice 28 days after CCl_4 treatment (Figure 8A+B). Similarly, the percentage of TUNEL-positive cells in WT and Jnk1$^{\Delta hepa}$ livers was 1.8±0.3 and 1.6±0.4, 28 days after BDL, respectively. In contrast, significantly lower TUNEL-positive cells (1.0±0.1) were found in Jnk1$^{-/-}$ livers (Figure 8C+D).

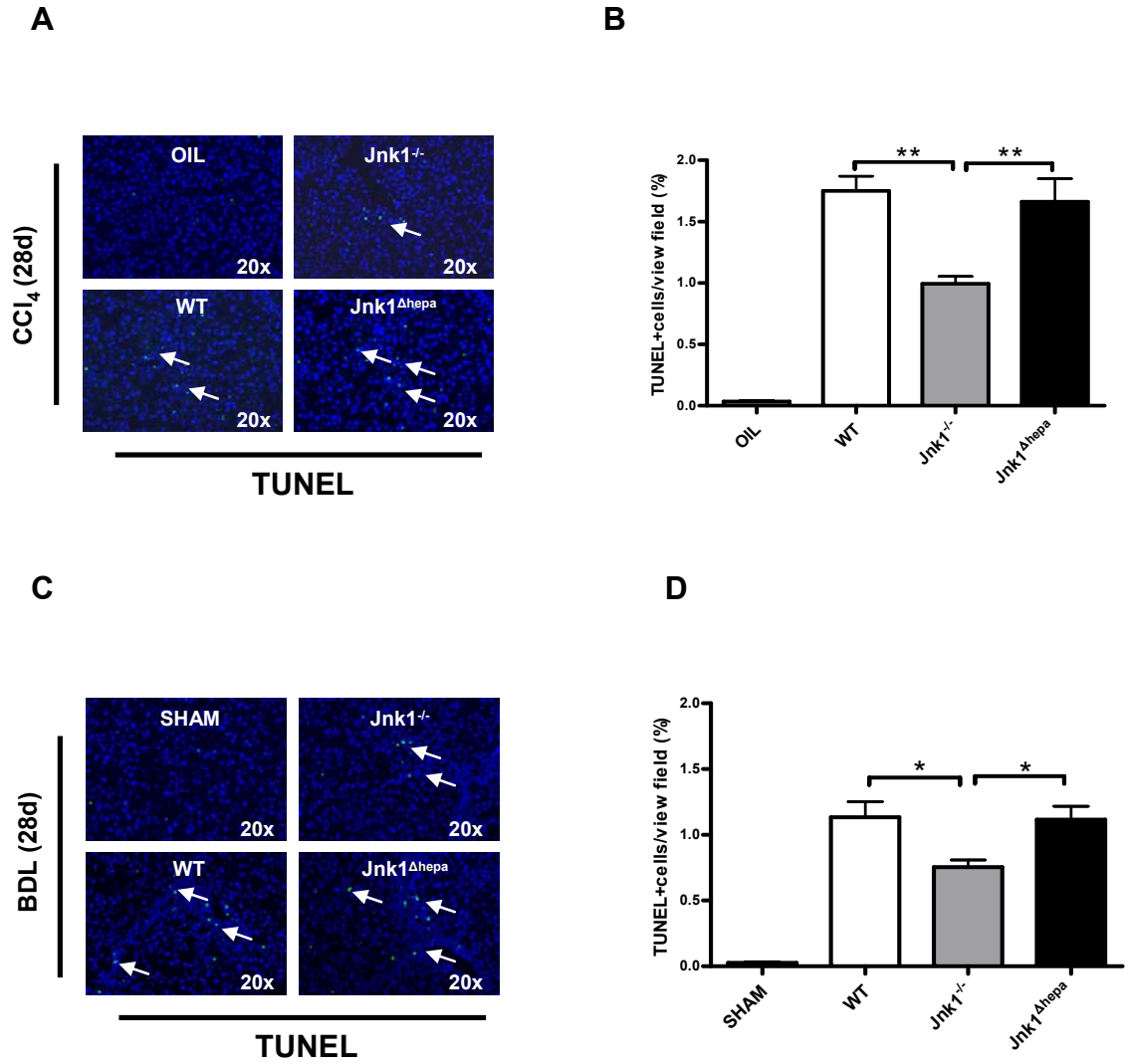

Figure 8. Analysis of apoptosis in livers from CCl_4- and BDL-treated mice. (A) Representative TUNEL stainings were performed on frozen liver sections after 4 weeks of repeated CCl_4 injections. **(B)** Quantification of TUNEL-positive cells in WT, Jnk1$^{-/-}$ and Jnk1$^{\Delta hepa}$ mice after 4 weeks of CCL_4 repeated injections. **(C)** Representative TUNEL stainings were performed on frozen liver sections after 4 weeks of BDL surgery. Arrows (↑) indicate TUNEL-positive cells. Values are mean ± SEM from at least 8-10 mice per time point. **(D)** Quantification of TUNEL-positive cells in WT, Jnk1$^{-/-}$ and Jnk1$^{\Delta hepa}$ after 4 weeks of BDL surgery are shown. Arrows (↑) indicate TUNEL-positive cells. Values are mean ± SEM from at least 8-10 mice per group (*p<0.05; **p<0.01; ***p<0.001).

3.2 JNK1 in NPCs determines hepatocyte proliferation after BDL and CCl_4 treatment.

Acute and chronic liver injury is followed by a phase of hepatocyte proliferation in order to restore liver mass [79]. Thus, we investigated changes in the expression of cell cycle markers. PCNA, Cyclin D and Cyclin A levels were strongly up-regulated in

Jnk1$^{\Delta hepa}$ and WT livers 4 weeks after BDL or after repetitive CCl_4 treatment, respectively (Figure 9). In contrast, these changes were significantly less severe in Jnk1$^{-/-}$ mice suggesting reduced compensatory proliferation after injury in both experimental models (Figure 9). These results were further corroborated at the mRNA level.

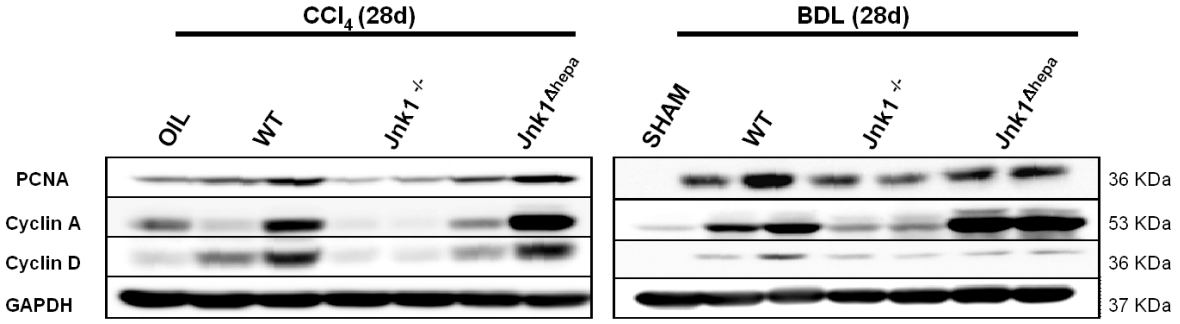

Figure 9. Expression of cell cycle markers of livers from CCl_4- and BDL-treated liver specimens. Liver extracts from WT, Jnk1$^{-/-}$ and Jnk1$^{\Delta hepa}$ mice sacrificed 28 days after CCl_4 treatment or BDL surgery.

PCNA and Cyclin D were highly expressed in Jnk1$^{\Delta hepa}$ and WT livers after chronic liver injury and significantly lower in Jnk1$^{-/-}$ mice (Figure 10A-D).

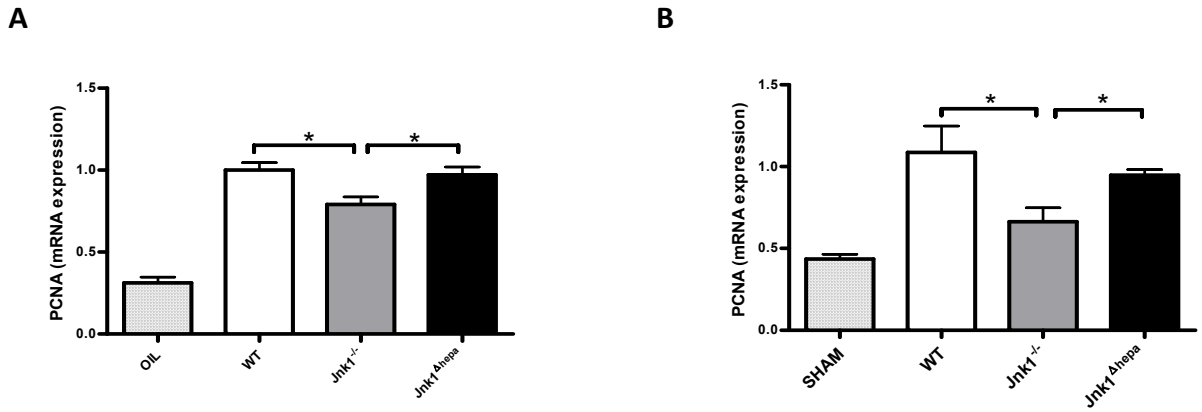

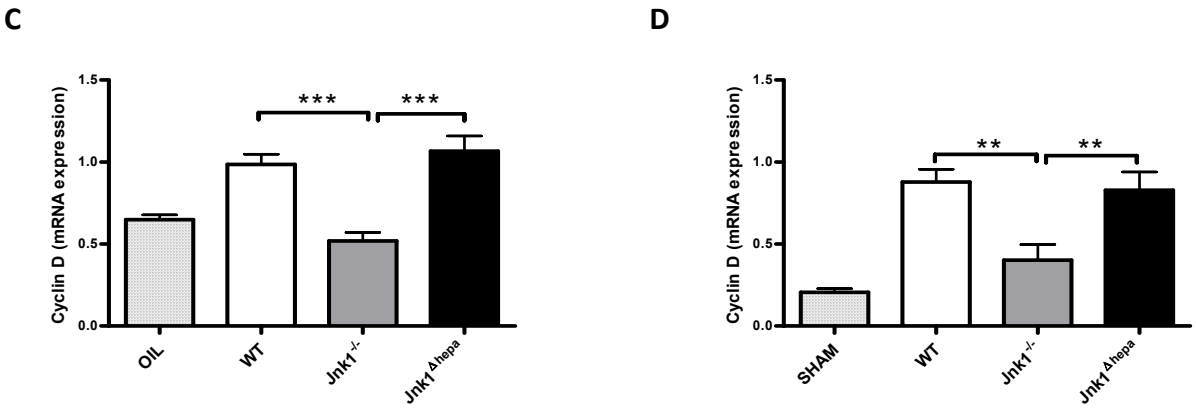

Figure 10. mRNA expression analysis of liver samples after CCl_4 and BDL treatment. The samples were subjected to RT-PCR to analyse the expression of PCNA in WT, $Jnk1^{-/-}$ and $Jnk1^{\Delta hepa}$ mice sacrificed 28 days after CCl_4 treatment **(A)** or BDL surgery **(B)**. The same samples were subjected to RT-PCR to analyse the expression of Cyclin D in WT, $Jnk1^{-/-}$ and $Jnk1^{\Delta hepa}$ mice sacrificed 28 days after CCl_4 treatment **(C)** or BDL surgery **(D)**. Values are mean ± SEM from at least 8-10 mice per group (**p<0.01***; p<0.001).

Moreover, quantification of cell proliferation with Ki-67 immunostaining demonstrated lower proliferation rates in $Jnk1^{-/-}$ compared with $Jnk1^{\Delta hepa}$ and WT livers treated with CCl_4 or with BDL for 4 weeks (Figure 11A+B).

A

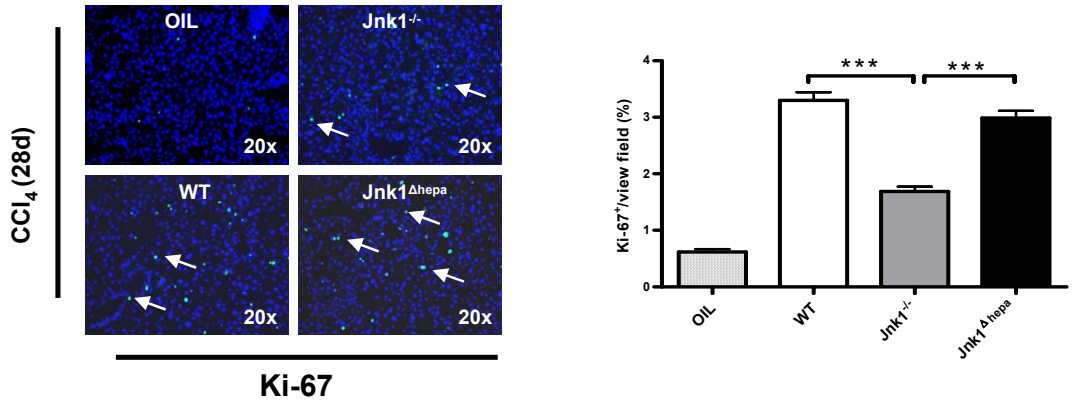

B

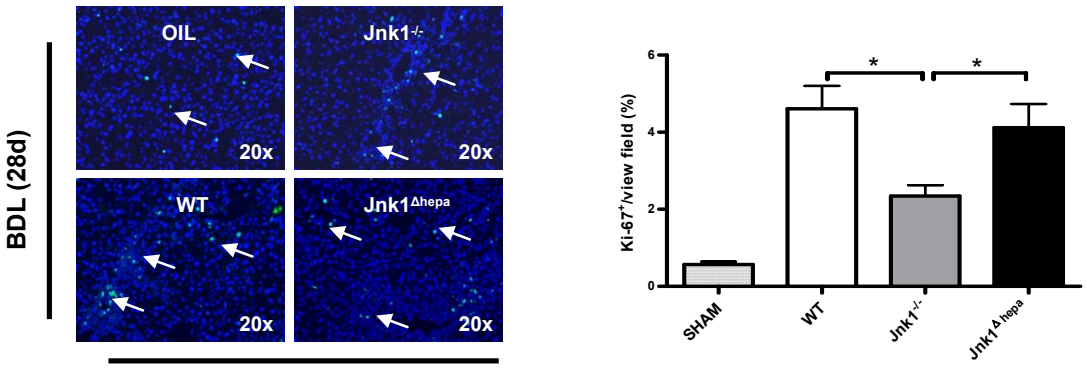

Figure 11. Cell proliferation analysis in liver after CCl_4 and BDL treatment. (A) Immunofluorescence staining for Ki-67 of liver cryosections after 4 weeks of repeated CCl_4 injections (left panels). The results were quantified and represented as percentage of area fraction. **(B)** Immunofluorescence staining for Ki-67 of liver cryosections after 4 weeks of BDL (left panels). The results were quantified using Image J Software, represented as percentage of Area Fraction. Arrows (↑) indicate Ki-67-positive cells. Values are mean ± SEM from at least 8-10 mice per group (*p<0.05; ***p< 0.001).

3.3 JNK1 in NPCs promotes liver fibrogenesis.

We next evaluated whether our findings were relevant for fibrosis progression and performed Sirius Red staining. Repeated CCl_4 injections induced severe collagen deposition and septum formation in $Jnk1^{\Delta hepa}$ and WT livers, classified by two independent pathologists as bridging fibrosis (Figure 12A). In contrast, quantification of Sirius Red staining revealed significantly lower collagen fibre formation in $Jnk1^{-/-}$ mice (Figure 12A+B). The essential role of JNK1 in non-hepatocytes for fibrosis progression was also found in the BDL model. JNK1 knockout livers showed reduced signs of fibrosis compared with $Jnk1^{\Delta hepa}$ and WT mice 4 weeks after BDL (Figure 12C+D).

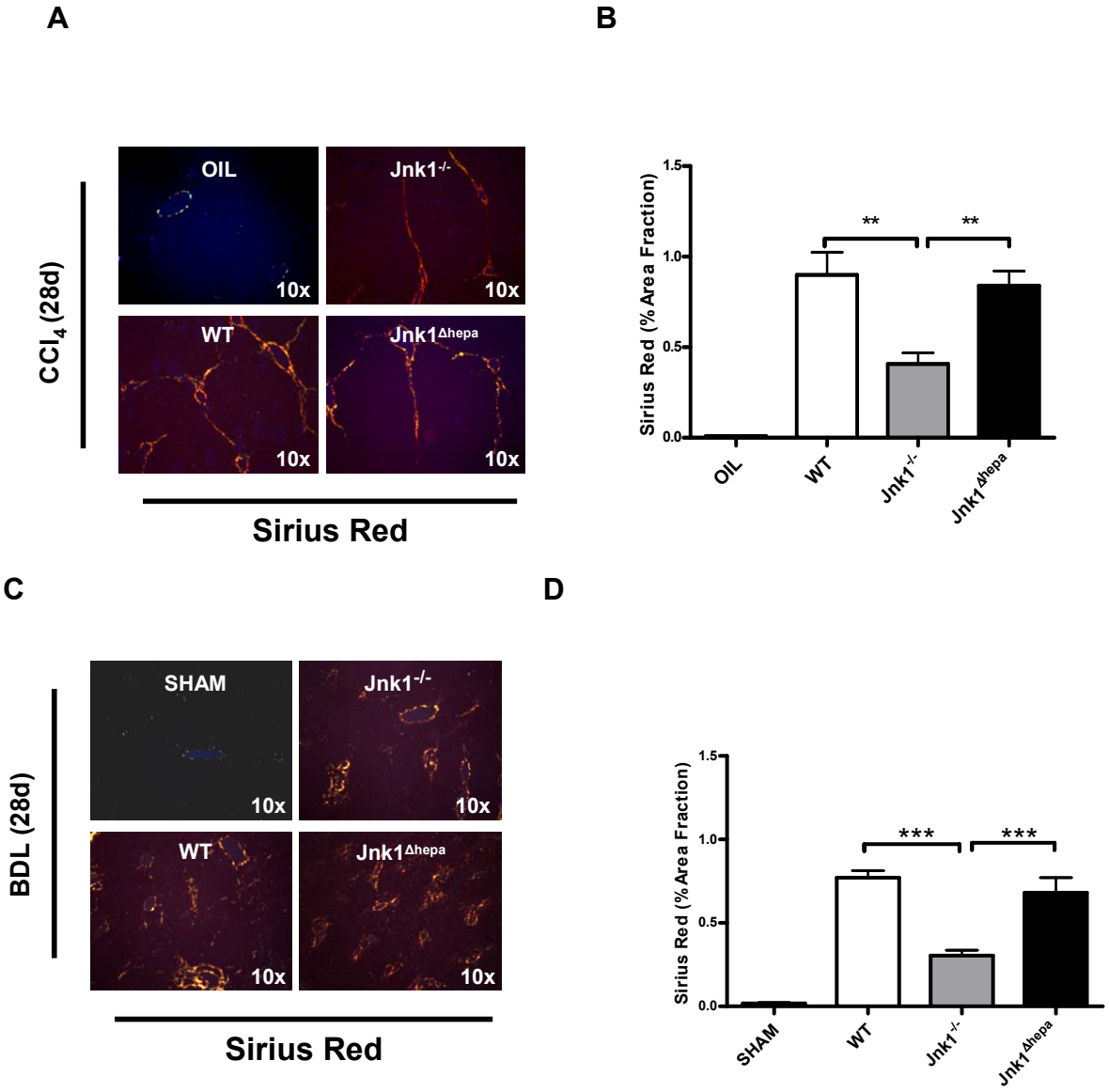

Figure 12. Sirius Red staining of liver samples after CCl_4 and BDL treatment. (A,C) Representative Sirius red staining of liver paraffin sections from WT, $Jnk1^{-/-}$ and $Jnk1^{\Delta hepa}$ after 4 weeks of CCl_4 treatment **(A)** or BDL **(C)**. **(B, D)** Sirius red staining were quantified using paraffin sections from WT, $Jnk1^{-/-}$ and $Jnk1^{\Delta hepa}$ livers after 4 weeks of CCl_4 treatment **(B)** or BDL **(D)**.

These findings were further validated by measuring α-SMA and Collagen IA1 mRNA and protein expression (Fig 13A-G). Conclusively, these findings strengthened our previous results as detected by Sirius Red staining. $Jnk1^{-/-}$ livers show reduced α-SMA and Collagen IA1 expression compared with $Jnk1^{\Delta hepa}$ and WT animals, in both experimental models.

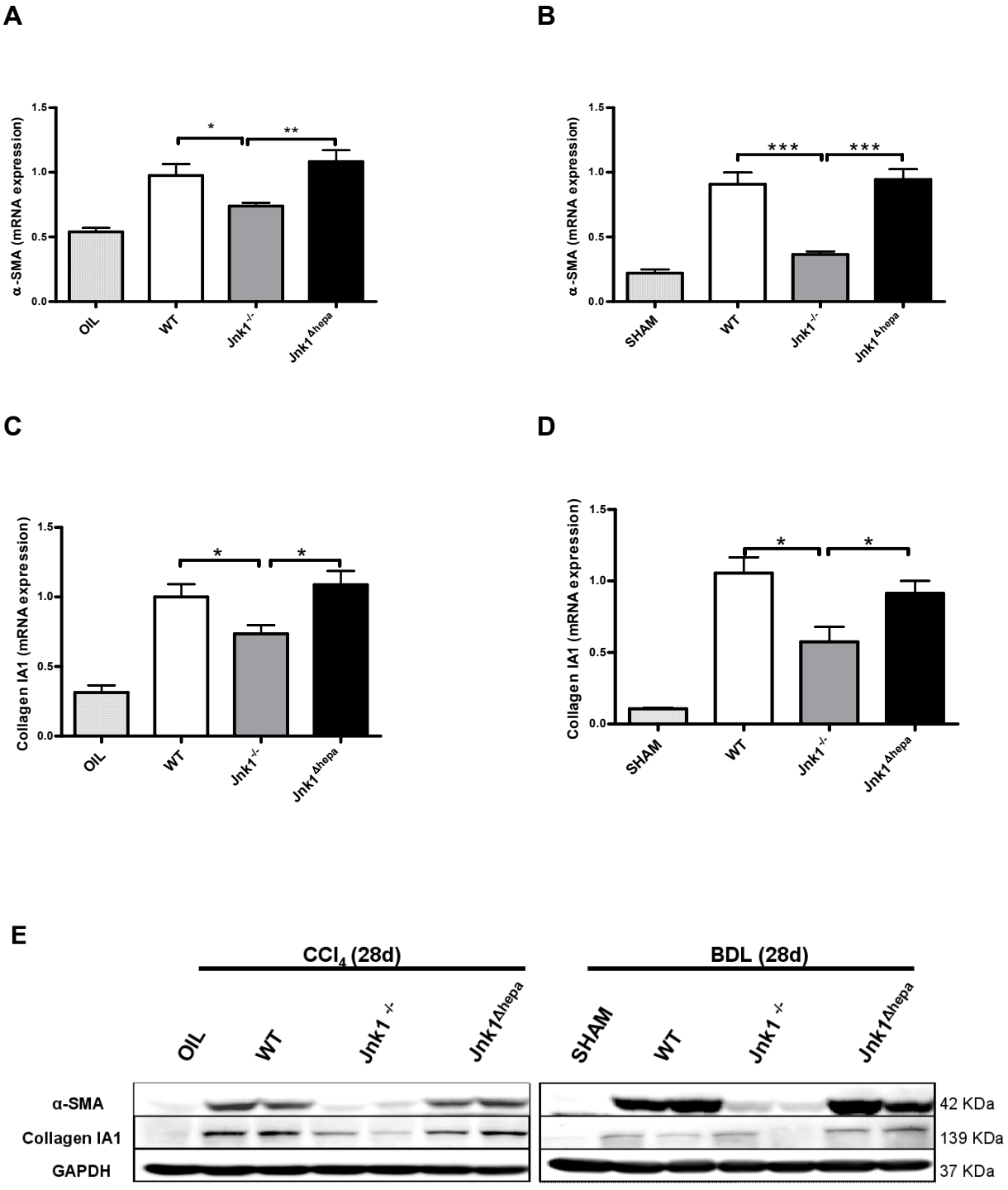
A
α-SMA (mRNA expression)
1.5
1.0
0.5
0.0
*
**
OIL
WT
Jnk1-/-
Jnk1Δhepa
B
α-SMA (mRNA expression)
***
***
SHAM
WT
Jnk1-/-
Jnk1Δhepa
C
Collagen IA1 (mRNA expression)
*
*
OIL
WT
Jnk1-/-
Jnk1Δhepa
D
Collagen IA1 (mRNA expression)
*
*
SHAM
WT
Jnk1-/-
Jnk1Δhepa
E
CCl4 (28d)
BDL (28d)
OIL
WT
Jnk1 -/-
Jnk1Δhepa
SHAM
WT
Jnk1 -/-
Jnk1Δhepa
α-SMA
Collagen IA1
GAPDH
42 KDa
139 KDa
37 KDa

F

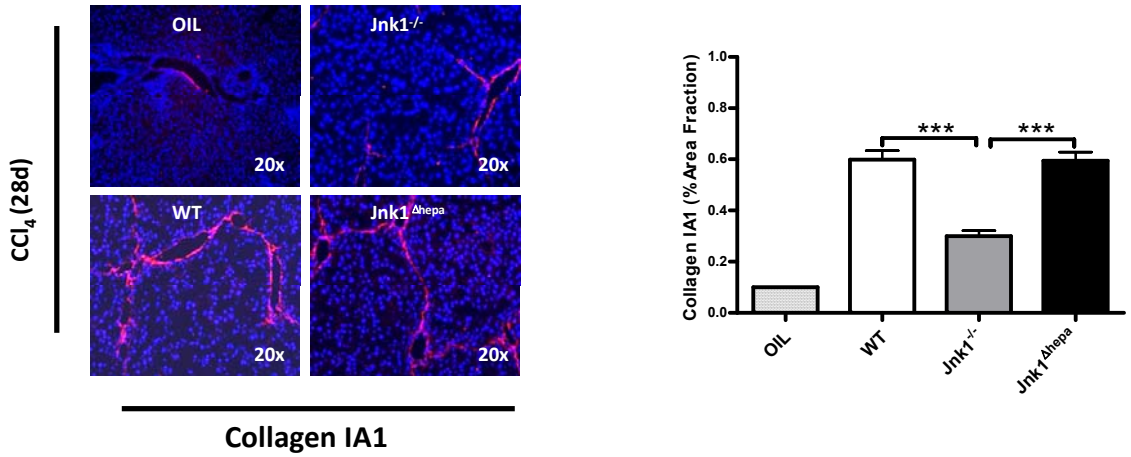

G

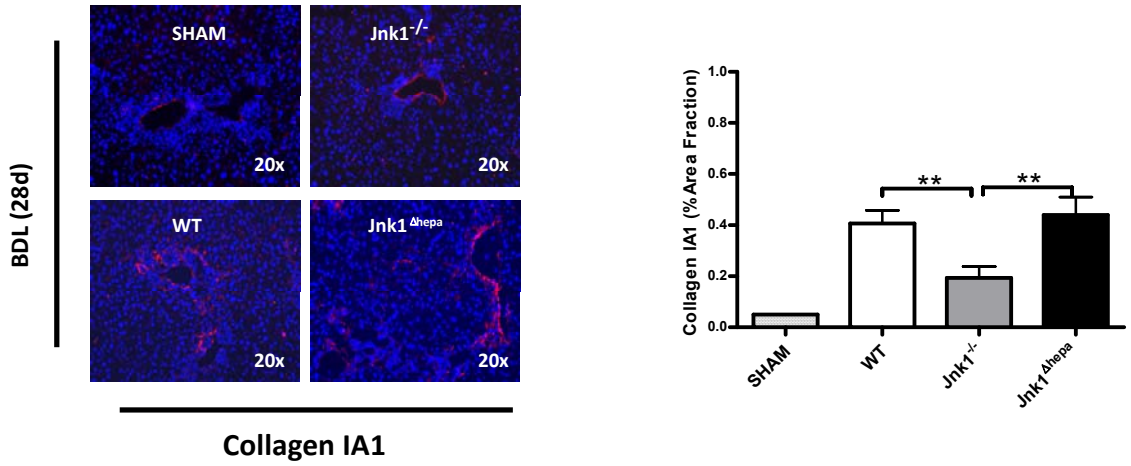

Figure 13. Liver fibrogenesis in liver after CCl_4 and BDL treatment. (A, B) mRNA expression analysis of α-SMA was quantified by RT-PCR of liver samples taken from WT, $Jnk1^{-/-}$ and $Jnk1^{\Delta hepa}$ mice sacrificed after after 4 weeks of chronic CCl_4 treatment **(A)** or BDL surgery **(B). (C, D)** mRNA expression analysis of Collagen IA1 was quantified by RT-PCR of liver samples taken from WT, $Jnk1^{-/-}$ and $Jnk1^{\Delta hepa}$ mice sacrificed 28 days after chronic CCl_4 treatment **(C)** or BDL **(D)**. Values are mean ± SEM from at least 8-10 mice per time point and condition. **(E)** Liver extracts from WT, $Jnk1^{-/-}$ and $Jnk1^{\Delta hepa}$ mice sacrificed 28 days after CCl_4 treatment or BDL surgery were examined by immunoblot analysis by probing with antibodies to α-SMA, Collagen IA1 and GAPDH as indicated. **(F, G)** Quantification was performed on Collagen IA1 staining frozen sections from livers of WT, $Jnk1^{-/-}$ and $Jnk1^{\Delta hepa}$ after 4 weeks of CCl_4 treatment **(F)** or BDL **(G)**. Values are mean ± SEM from at least 8-10 mice per group (*p<0.05; **p<0.01; ***p<0.001).

3.4 The WT recipient genotype after BMT determines the degree of liver injury.

Our results demonstrate that JNK1 is crucial for liver fibrogenesis, but other cells rather than hepatocytes are relevant in mediating fibrosis. Hence we next investigated whether BMCs are essential in promoting liver fibrosis. We thus performed BMT experiments. WT and Jnk1$^{-/-}$ mice were lethally irradiated and reconstituted with either Jnk1$^{-/-}$ or WT bone marrow (BM). Five weeks after BMT, recipient mice were subjected to chronic CCl_4 or BDL treatment for 28 days (Figure 14A). 5 weeks after BMT, chimerism in the liver was confirmed by PCR which demonstrated successful BM reconstitution (Figure 14B).

A

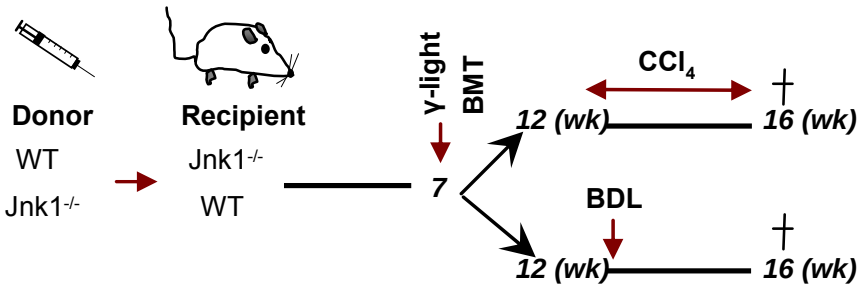

B

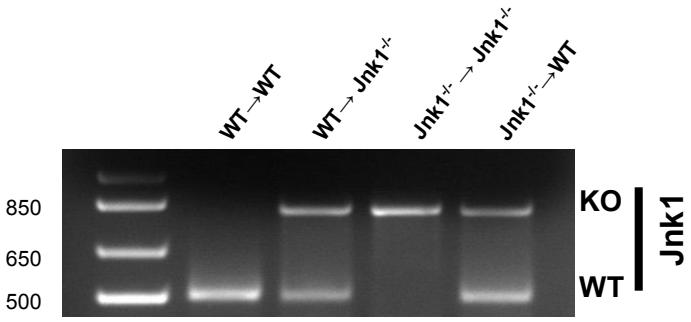

Figure 14. Schematic diagram of BMT and proof of BM reconstitution. (A) Scheme of the chimeras used for radiation and the experimental design of the study. **(B)** Liver DNA was prepared and PCR was performed from mice 9 weeks after BMT. The JNK1-specific bands for wt and JNK1$^{-/-}$ are indicated confirming successful chimerism in the liver after BMT.

No apparent macroscopic differences were found between chimeric mice treated with repetitive doses of CCl_4 for 4 weeks (Figure 15A). Histological analysis showed

no difference in hepatocellular damage but more infiltration of inflammatory cells in WT recipients transplanted with Jnk1$^{-/-}$ mice (Jnk1$^{-/-}$→WT) (Figure 15B).

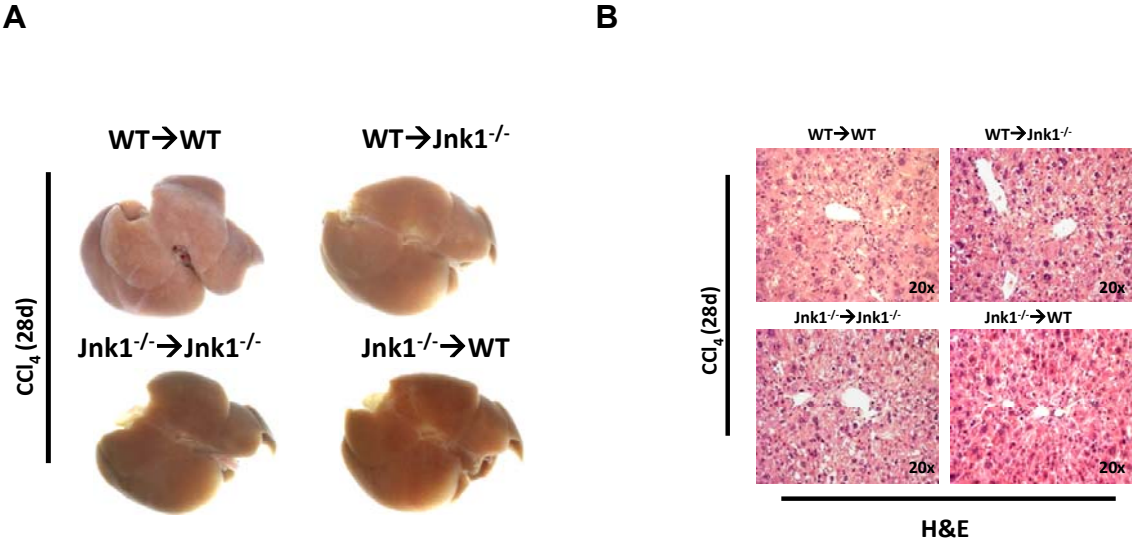

Figure 15. Macroscopic appearance and H&E staining of livers from CCl$_4$-treated mice after BMT. (A) Macroscopic appearance of livers of WT or Jnk1$^{-/-}$ mice transplanted with Jnk1$^{-/-}$ or WT bone marrow cells. 5 weeks later mice were treated with CCl_4 for a period of 4 weeks. **(B)** Representative H&E staining of liver sections from these mice are shown.

The BDL treated chimeric WT mice reconstituted with WT (WT→WT) and Jnk1$^{-/-}$ BM (Jnk1$^{-/-}$→WT) showed macroscopically yellowish dots on their surface (Figure 16 A+B). In contrast, Jnk1$^{-/-}$ recipients transplanted with WT or Jnk1$^{-/-}$ BM (WT/Jnk1$^{-/-}$ →Jnk1$^{-/-}$) showed no external signs of liver injury (Figure 16A+B).

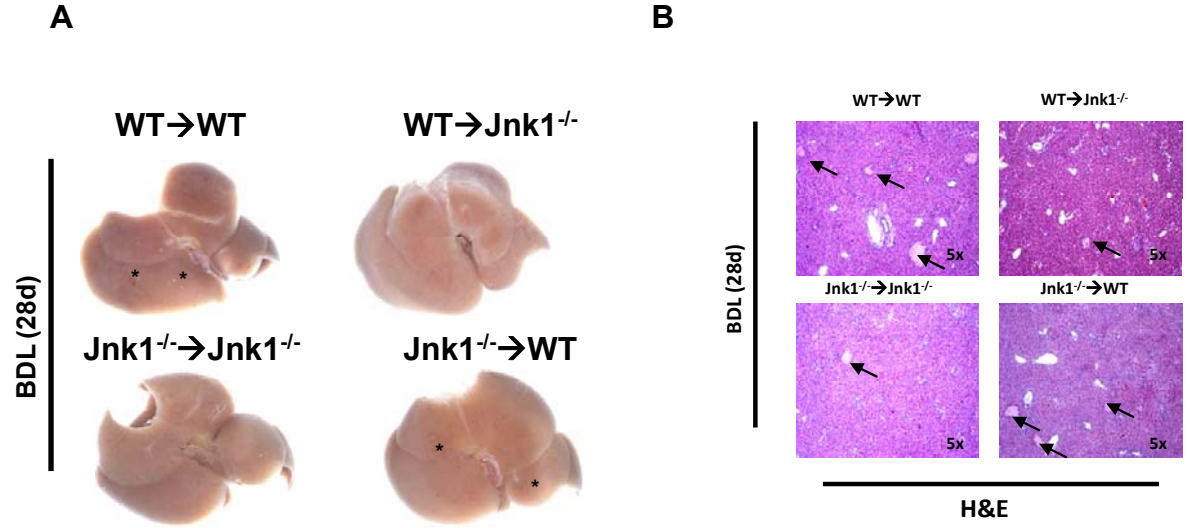

Figure 16. Presence of necrotic foci and biliary infarcts of BDL-subjected liver specimens after BMT. (A) Macroscopic appearance of livers of WT or Jnk1$^{-/-}$ mice transplanted with Jnk1$^{-/-}$ or WT bone marrow cells are shown. 5 weeks after BMT mice were subjected to BDL and were sacrificed 28 days later. (*) indicates yellow dots on the liver surface. **(B)** Representative H&E staining of liver sections

from these mice. (↑) Bile infarcts corresponding to the yellow dots observed on the liver surface and histologically assigned as necrotic foci by an expert liver pathologist.

Histological analysis of BDL-treated livers showed necrotic foci in WT recipient mice reconstituted with Jnk1$^{-/-}$ BM (Jnk1$^{-/-}$→WT) or WT BM (WT→WT) indicative of hepatocellular damage (Figure14 A,B). In contrast, Jnk1$^{-/-}$ mice reconstituted with either Jnk1$^{-/-}$ BM (Jnk1$^{-/-}$→Jnk1$^{-/-}$) or WT BM (WT→Jnk1$^{-/-}$) displayed presence of inflammatory cells and some ductular proliferation but significantly lower hepatic cell death compared with the WT recipient groups (Figure 17A,B). Along with these results, plasma AST (Figure 17C), ALT, Bilirubin and AP (Figure 17D-F) levels evidenced significantly higher liver damage after BDL in WT mice reconstituted with WT BM (WT→WT) or Jnk1$^{-/-}$ BM (Jnk1$^{-/-}$→WT).

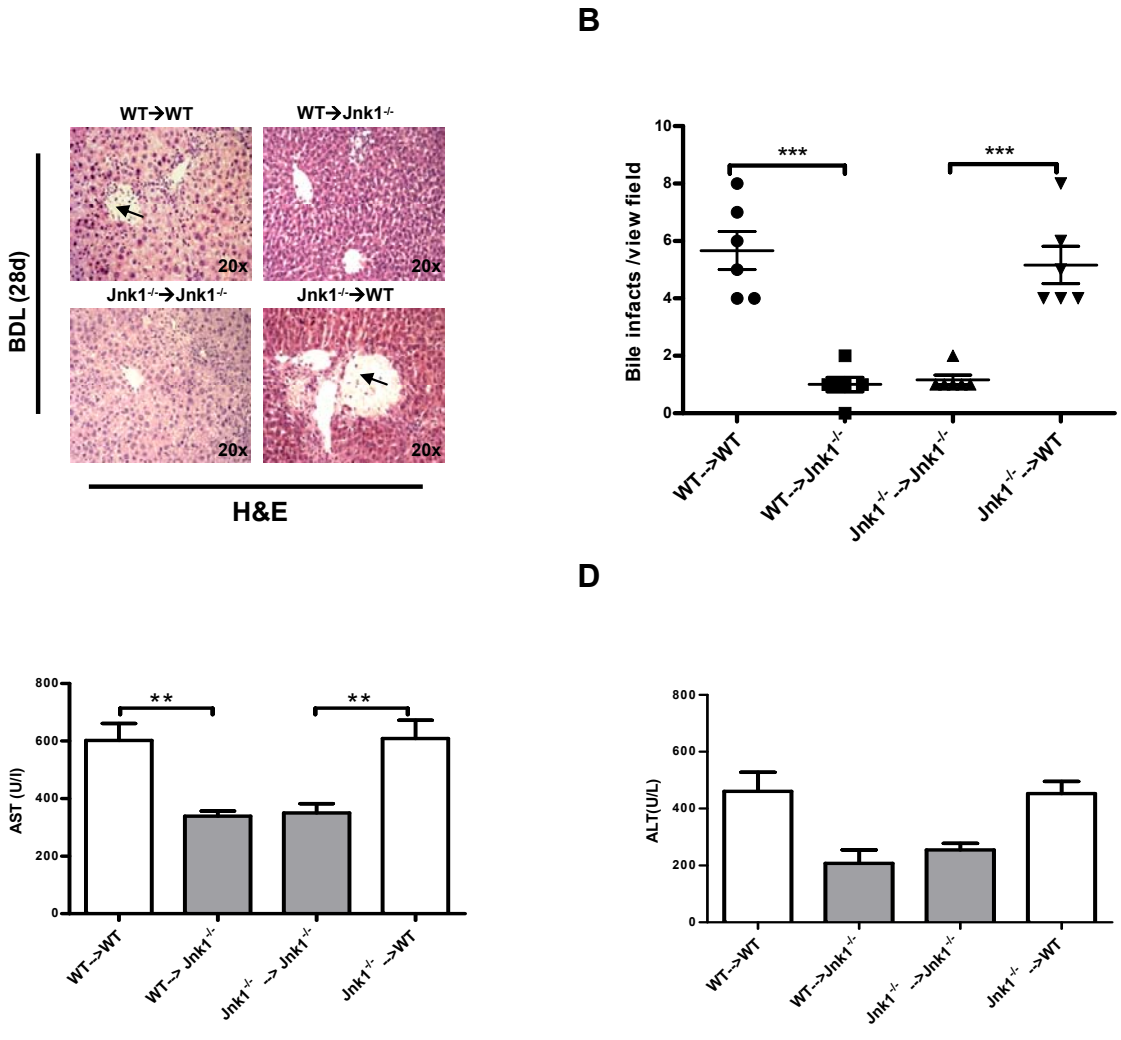

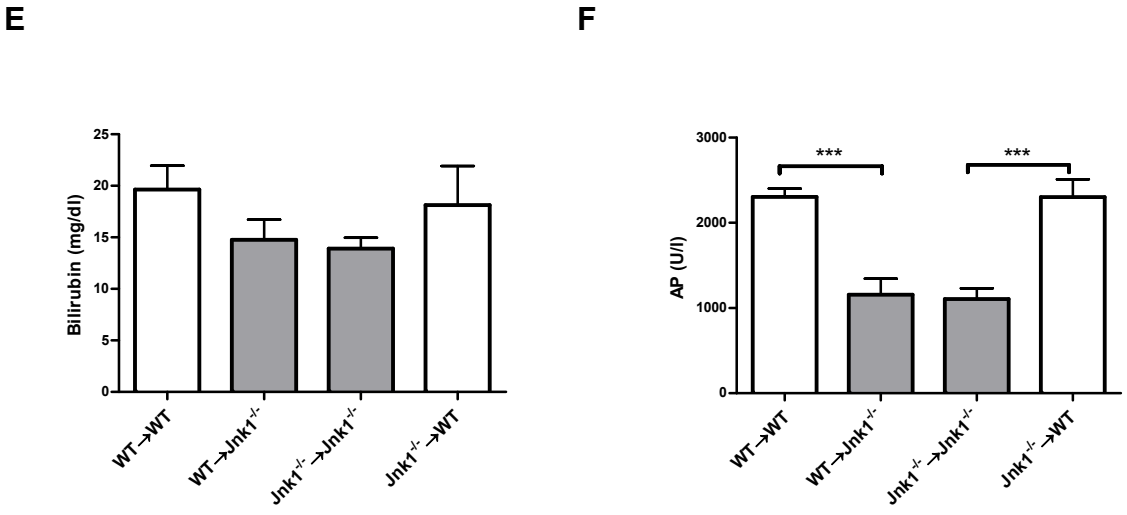

Figure 17. Liver injury in BDL-subjected liver specimens after BMT. (A) Representative H/E staining of necrotic foci from WT and Jnk1$^{-/-}$ mice transplanted with Jnk1$^{-/-}$ or WT bone marrow cells and subjected to BDL for 4 weeks showing areas of necrotic foci (*). **(B)** Quantification of bile infarcts of WT and Jnk1$^{-/-}$ mice transplanted with Jnk1$^{-/-}$ or WT bone marrow cells treated with BDL for 28 days, was performed blinded by a pathologist. **(C-F)** Serum levels of AST **(C)**, ALT **(D)**, Bilirubin **(E)** and AP **(F)** were determined after BMT + BDL in Jnk1$^{-/-}$ or WT mice. Values are mean ± SEM from at least 6-8 mice per group (**p<0.01; ***p<0.001).

3.5 JNK1 in bone marrow derived cells has no relevance for liver fibrogenesis.

Our first findings with BMT experiments revealed that BM-derived cells of WT or Jnk1$^{-/-}$ transplanted into WT or Jnk1$^{-/-}$ mice have no major impact on the injury phenotype of the livers of the respective recipients. Thus, we next studied how BMT affected liver fibrogenesis and analyzed matrix formation by Sirius red staining and quantified these results by ImageJ software (Figure 18A+B). Consistently, in both experimental models our observations showed that WT animals reconstituted with WT or Jnk1$^{-/-}$ BM showed more matrix deposition compared with Jnk1$^{-/-}$ mice reconstituted with Jnk1$^{-/-}$ or WT BM (Figure 18A+B). Accordingly, this analysis showed that the JNK1-dependent effect on liver fibrogenesis is primarily determined by non-BM derived cells.

In order to further support this observation, we performed Collagen IA1 protein immunostaining in the livers of the different groups after BMT followed by repetitive CCl_4 treatment or BDL (Figure 18C+D). These results also demonstrated that the reconstituted WT recipient mice had significantly more Collagen IA1 deposition

compared with the chimeric Jnk1$^{-/-}$ animals. Therefore, the BMT experiments showed that the JNK1 status in BM-derived cells is of minor relevance for liver fibrogenesis in the BDL and the CCl_4 model.

A

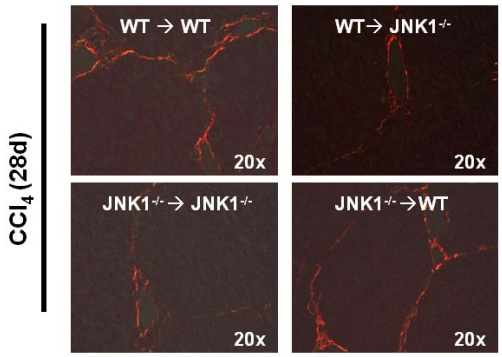

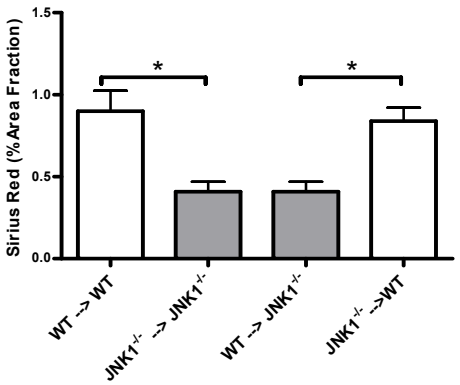

B

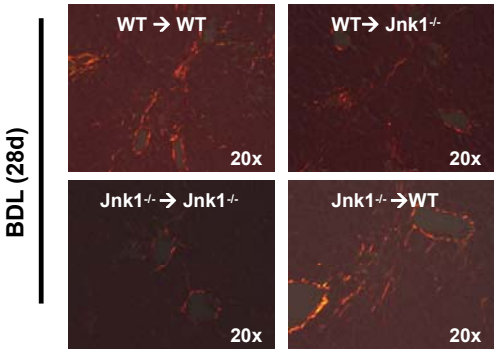

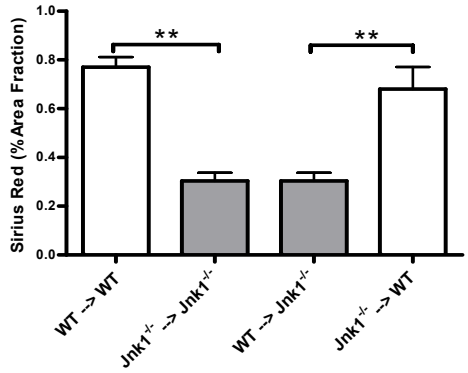

C

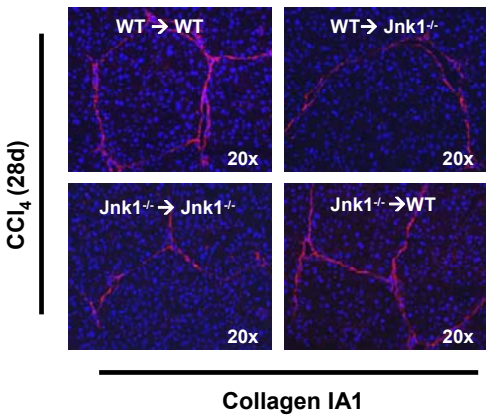

D

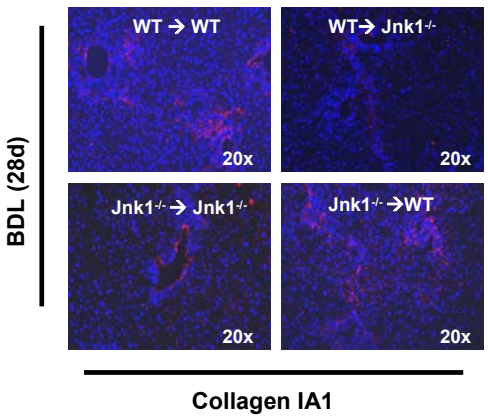

Figure 18. Liver fibrogenesis analysis in chimeric liver samples after CCl_4 and BDL. (A, B) Representative Sirius red staining of liver paraffin sections from WT or Jnk1$^{-/-}$ mice transplanted with Jnk1$^{-/-}$ or WT bone marrow cells and subjected to CCl_4 treatment **(A)** of BDL **(B)** for 4 weeks. (left panels). Quantification of the same samples is represented as positive area fraction of Sirius red staining(right panel). **(C, D)** Representative Collagen IA1 staining of liver frozen sections from WT or Jnk1$^{-/-}$ mice transplanted with Jnk1$^{-/-}$ or WT bone marrow cells and subjected to CCl4 treatment **(C)** or BDL **(D)** for 4 weeks. Values are mean ± SEM from at least 7 mice per group (*p<0.05; **p<0.01).

3.6 Array analysis suggests that genes involved in matrix formation are decreased in Jnk1$^{-/-}$ mice.

As our results suggested that other cells than BM-derived cells or hepatocytes are involved in mediating the pro-fibrogenic JNK1-dependent effect, we performed array analysis to potentially link the gene profile to a specific liver cell type. We applied microarray analysis to detect changes in mRNA expression between WT, Jnk1$^{-/-}$ and Jnk1$^{\Delta hepa}$ (Figure 19). We calculated the average expression of the sham-operated mice and divided the log2 values of the individual mice by the mean of the sham. Log ratios were saved in a txt file and analyzed with the Multiple Experiment Viewer. First we selected the top 1000 variable genes in the dataset based on interquartile range and then selected genes associated with HSCs activation and hepatic fibrosis. A representative sample of these genes was then hierarchically clustered and statistically analyzed by Pearson correlation. The results as depicted in Figure 19 showed that genes involved HSCs activation, hepatic fibrosis and liver damage exhibit major changes between the knockout strains. HSCs-marker genes such as *raet1d* (retinoic acid early transcript-delta), or genes associated with hepatic fibrosis such as *mmd2* (monocyte to macrophage differentiation-associated 2), *gas1* (growth arrest specific-1), and *grem1* (gremlin), *timp4* (tissue inhibitor metalloproteinase-4) or *mmp7* (matrix metalloproteinase-7) were differentially clustered according to fold change. These genes were down-regulated in Jnk1$^{-/-}$ compared with WT and Jnk1$^{\Delta hepa}$ livers. Of notice, genes related to protection against fibrosis such as *saa1* (serum amyloid-1) or *saa2* (serum amyloid-1) were highly up-regulated in Jnk1$^{-/-}$ and strongly down-regulated in Jnk1$^{\Delta hepa}$ mice (Figure 19). Therefore, our microarray data suggested that genes directly involved in matrix production showed specific differences in Jnk1$^{-/-}$ compared with Jnk1$^{\Delta hepa}$ and WT livers 28 days after BDL.

A

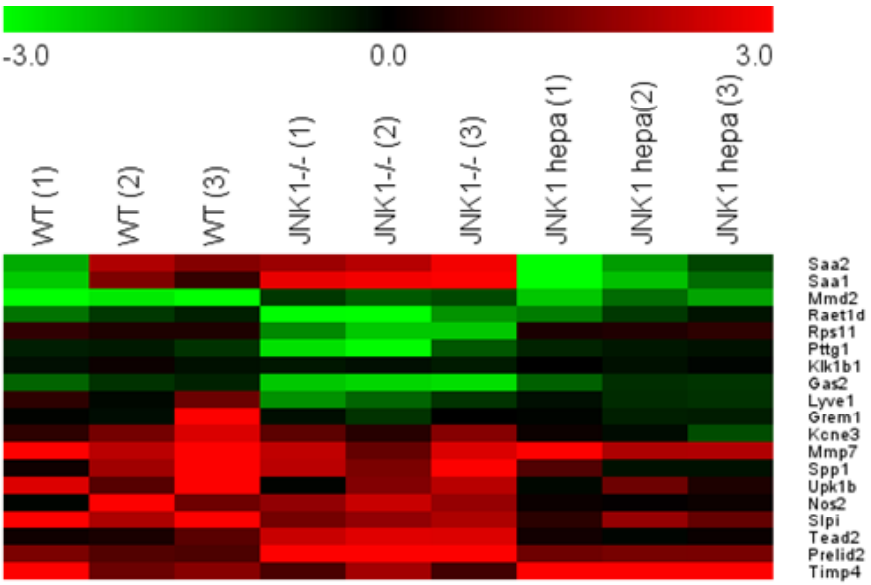

Figure 19. Microarray showing genes involved in matrix formation and deposition are decreased in Jnk1$^{-/-}$ mice. Microarray was performed in WT, Jnk1$^{-/-}$ and Jnk1$^{\Delta hepa}$; log2 expression values of the individual mice, were divided by the mean of the sham operated mice. Log ratios were saved in a txt file and analyzed with the Multiple Experiment Viewer. The selected up- and down-regulated genes are shown (RED: Up-regulated; GREEN: Down-regulated, n=3, fold change -3.0-3.0).

Microarray analysis suggested that cells directly involved in matrix production are associated with reduced fibrosis in Jnk1$^{-/-}$ livers. We thus analyzed α-SMA expression in liver paraffin sections to study HSCs activation during liver injury (Figure 20A+B). We found that lobular activated α-SMA HSCs in Jnk1$^{-/-}$ mice were less in number compared to WT and Jnk1$^{\Delta hepa}$ mice and that the septa are more slender, 28 days after CCl_4 treatment (Figure 20A). Indeed, α-SMA positive activated HSCs were observed in a perisinusoidal pattern forming fine portal-central septa (Figure 20A). Moreover, 28 days after BDL, α-SMA positive cells were mainly portal myofibroblasts, surrounding ductular proliferation areas (Figure 20B). Periportal fibrosis and portal-portal septa were formed in WT and Jnk1$^{\Delta hepa}$ mice and significantly reduced in Jnk1$^{-/-}$ livers (Figure 20B), suggesting that HSCs are directly involved in mediating the JNK1-dependent pro-fibrogenic effect on liver fibrogenesis.

Additionally, we performed CK19 staining in liver sections to investigate the pattern of ductular reaction during BDL-triggered liver injury (Figure 20C). WT and

Jnk1$^{\Delta hepa}$ mice exhited larger extension of the portal tract compared to the Jnk1$^{-/-}$ mice. Moreover, necrotic areas and periportal CK19 positive hepatocytes, a sign of periportal cholatestasis, were present in WT and Jnk1$^{\Delta hepa}$ mice but not in Jnk1$^{-/-}$ mice (Figure 20C).

A

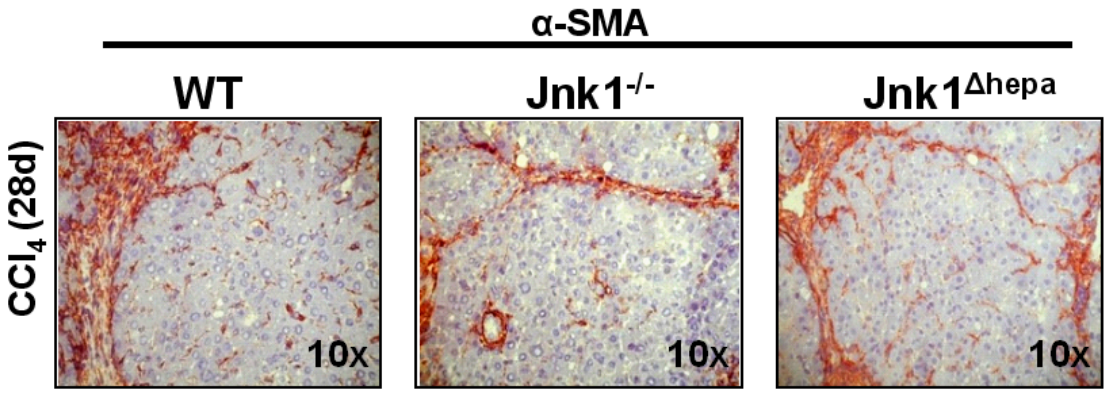

B

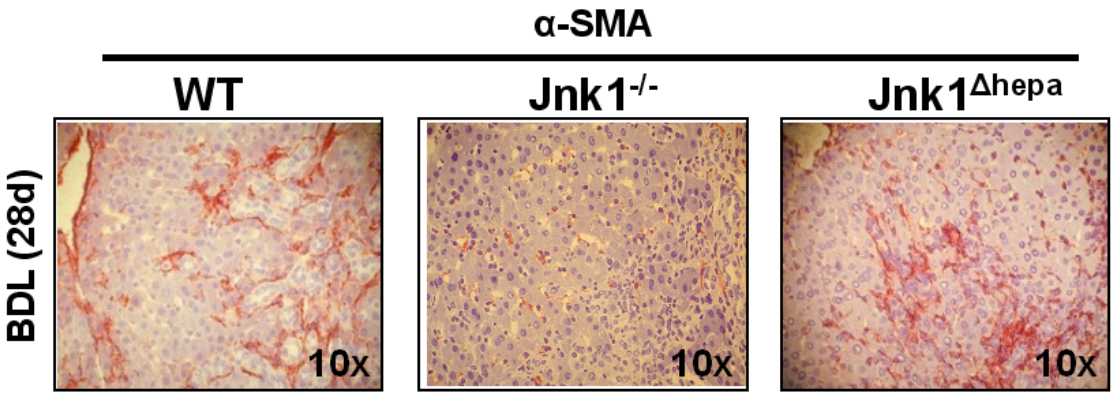

C

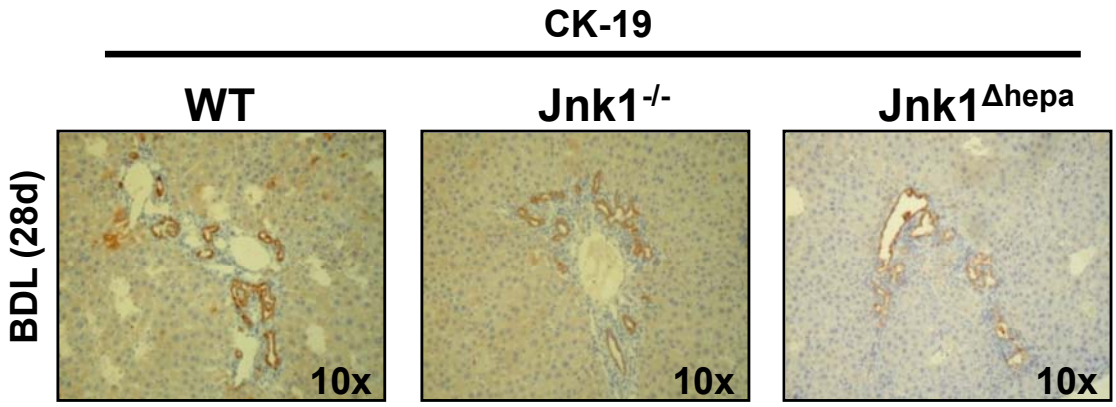

Figure 20. Activated HSCs analysis *in vivo* of liver samples after CCl_4 and BDL. (A, B) Immunohistochemistry was performed on liver paraffin sections for α-SMA in livers of WT, $Jnk1^{-/-}$ and $Jnk1^{\Delta hepa}$ mice, 28 days after CCl_4 **(A)** or BDL treatment **(B)**. **(C)** Immunohistochemistry staining on liver paraffin sections for CK-19 in livers of WT, $Jnk1^{-/-}$ and $Jnk1^{\Delta hepa}$ mice, 28 days after BDL treatment.

3.7 JNK1 is essential for HSCs transdifferentiation.

The array analysis and immunohistochemistry strongly suggested that differences in HSCs activation are found during chronic liver injury. We thus tested the importance of Jnk1 for HSCs transdifferentiation into myofibroblasts. Primary HSCs from WT, $Jnk1^{-/-}$ and $Jnk1^{\Delta hepa}$ mice were isolated using a FACSAria based protocol (Figure 21A). In these cells proliferation, apoptosis and transdifferentiation was studied *in vitro* over a time period of 10 days. We first studied p-JNK and α-SMA expression in WT HSCs. Our results clearly showed that transdifferentiation and α-SMA expression was associated with JNK activation (Figure 21B).

A

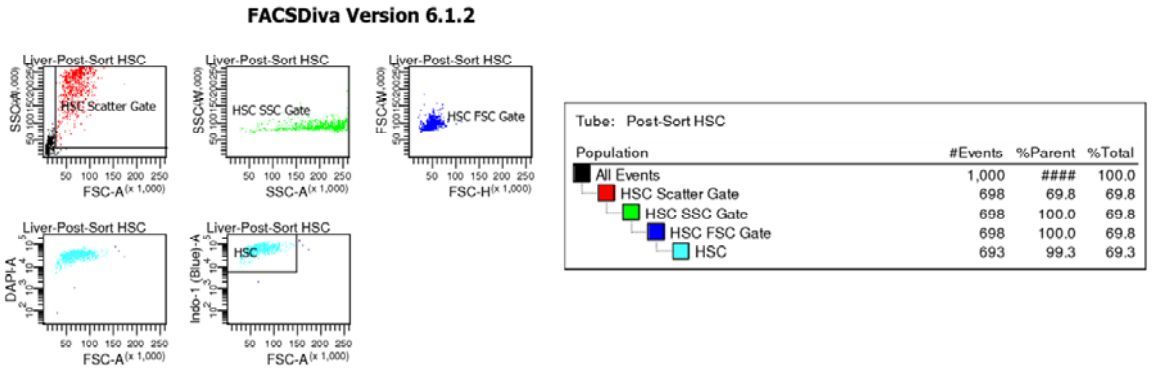

B

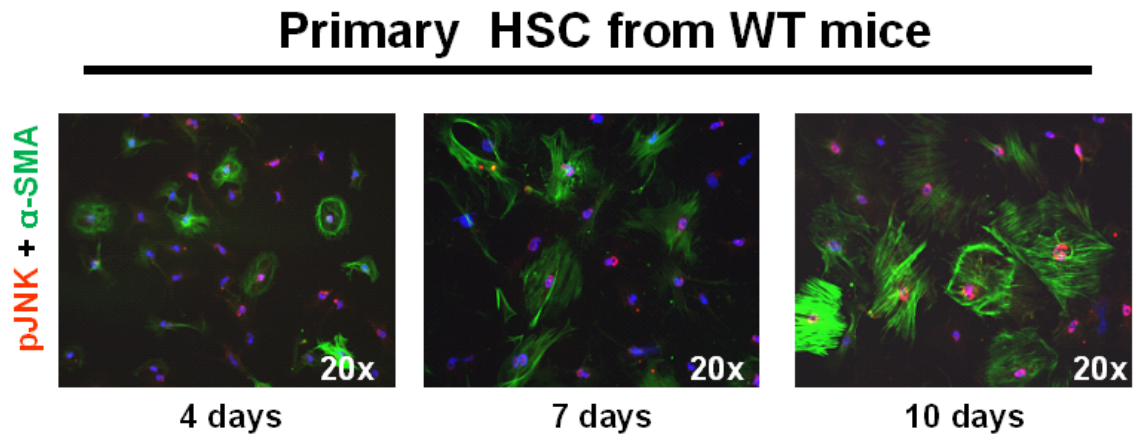

Figure 21. JNK1 in HSCs is essential for the pathogenesis of liver fibrosis. Primary HSCs were isolated from WT, Jnk1$^{-/-}$ and Jnk1$^{\Delta hepa}$ mice. A total number of 150.000 cells were seeded in 6-well plates and cultivated for up to 10 days. **(A)** Gating strategy in the Cell Sorter FACSAria for the isolation of primary HSCs **(B)** Co-immunofluorescence staining for pJNK (red) and α-SMA (green) was performed in WT cells from day 4 to day 10 after isolation.

Next, we quantified the total number of HSCs up to 10 days after isolation. The total number of living WT and Jnk1$^{\Delta hepa}$ HSCs increased continuously up to 10 days whereas proliferation in Jnk1$^{-/-}$ HSCs was significantly attenuated (Figure 22A). These differences of HSC proliferation were further strengthened using immunofluorescence stainings for Ki-67 and α-SMA. HSCs derived from Jnk1$^{-/-}$ mice showed significantly less Ki-67- and α-SMA-positivity compared with HSCs derived from WT or Jnk1$^{\Delta hepa}$ animals (Figure 22A+B).

A

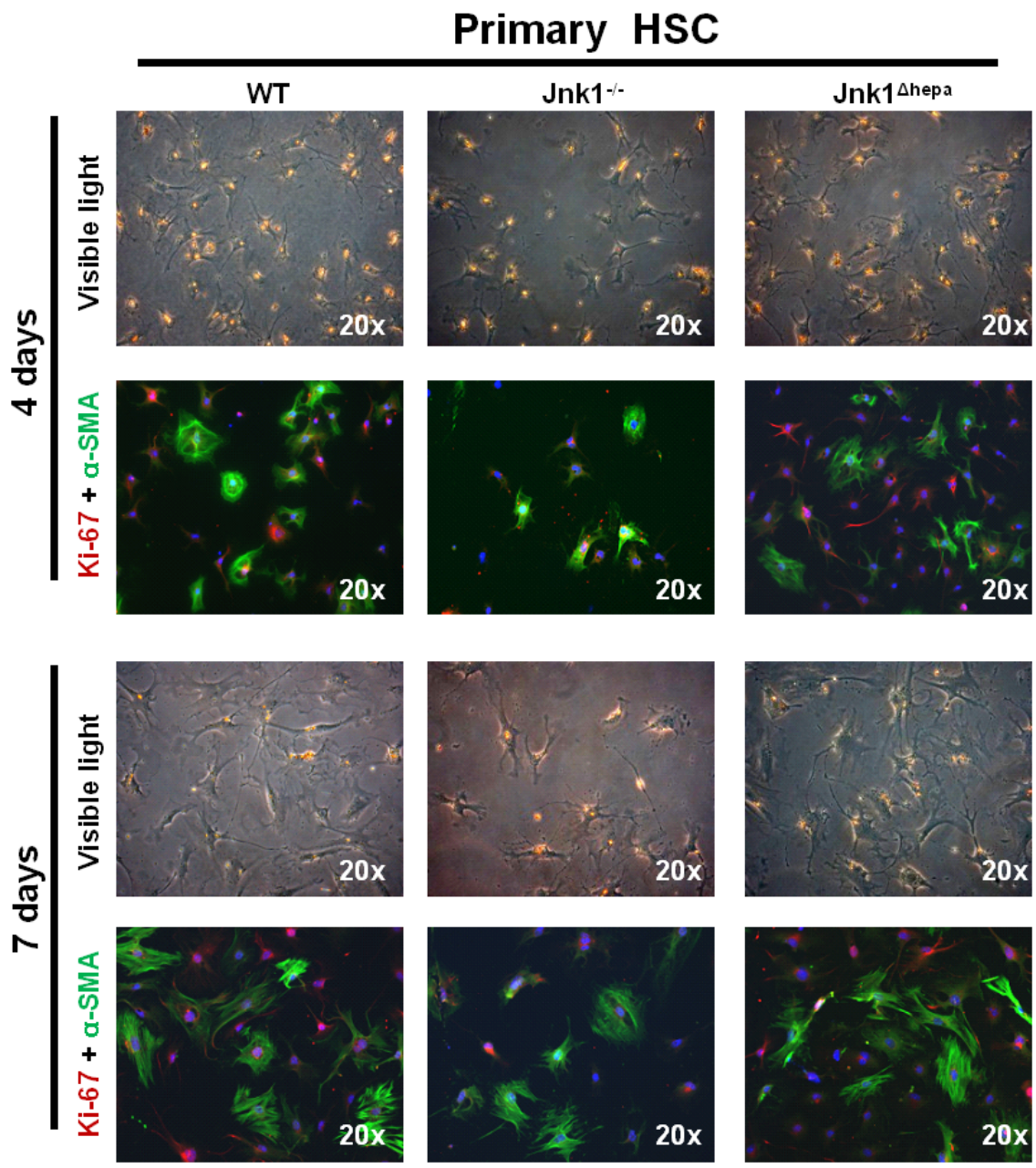
Primary HSC
WT
Jnk1-/-
Jnk1Δhepa
4 days
7 days
Visible light
Ki-67 + α-SMA
20x

B

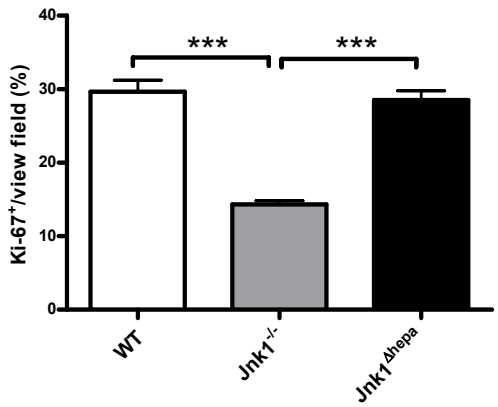
Ki-67+/view field (%)
40
30
20
10
0
***
***
WT
Jnk1-/-
Jnk1Δhepa

Figure 22. JNK1 in HSCs is essential for their proliferation. (A) Morphology and cell density was confirmed by phase contrast microscopy at day 4 and day 7 after isolation. Jnk1$^{-/-}$ HSCs was significantly attenuated (upper middle panels).Primary HSCs from WT, Jnk1$^{-/-}$ and Jnk1$^{\Delta hepa}$ mice were co-stained for Ki-67 and α-SMA at day 4 and day 7 after isolation. **(B)** mRNA expression analysis of Collagen IA1 Primary HSCs from WT, Jnk1$^{-/-}$ and Jnk1$^{\Delta hepa}$ mice were quantified for Ki-67 positive cells after 7 days in culture.

Additionally, we performed TUNEL analysis of seeded HSCs up to 10 days after isolation. In these experiments HSCs derived from Jnk1$^{-/-}$ livers showed more cell death compared with Jnk1$^{\Delta hepa}$ cells or WT cells (Figure 23A+B).

Subsequently, we quantified mRNA expression of α-SMA, Collagen IA1 and PDGF-Rβ (Figure 23C-E), known to be activated during HSCs transdifferentiation. HSCs from Jnk1$^{-/-}$ mice showed down-regulation of α-SMA, Collagen IA1 and PDGFR-β compared with WT and Jnk1$^{\Delta hepa}$ -derived HSC (Figure 23C-E). Altogether, the *in vitro* experiments with primary HSCs confirmed the in vivo studies defining JNK1 as an essential factor involved in HSCs activation and transdifferentiation.

A

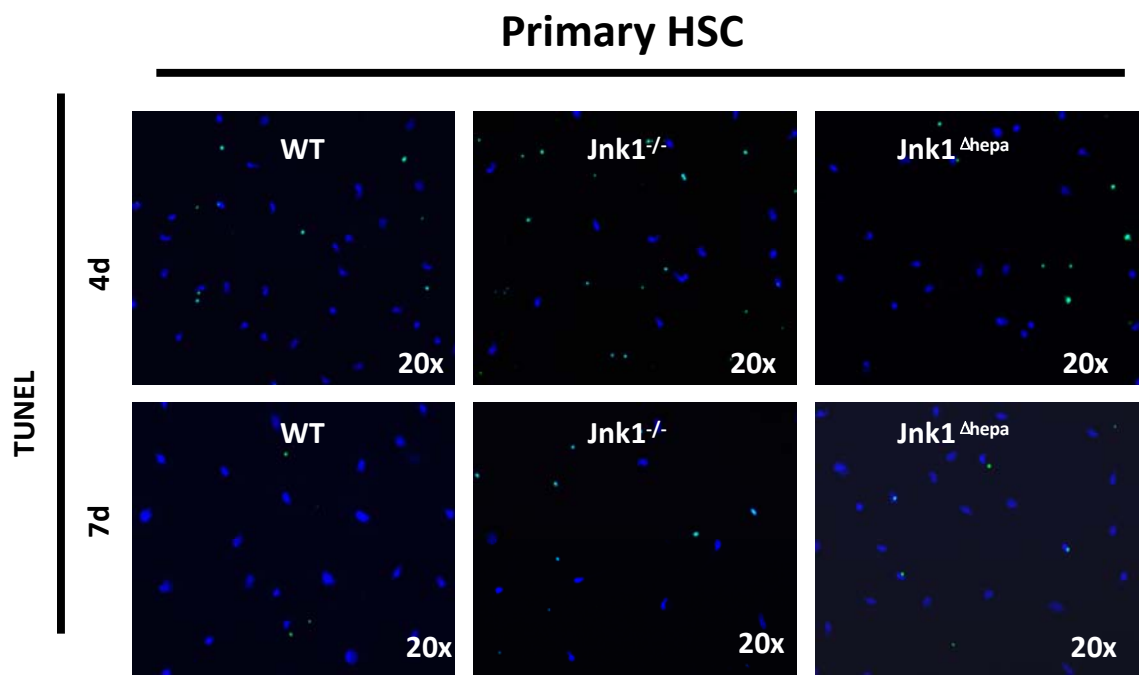

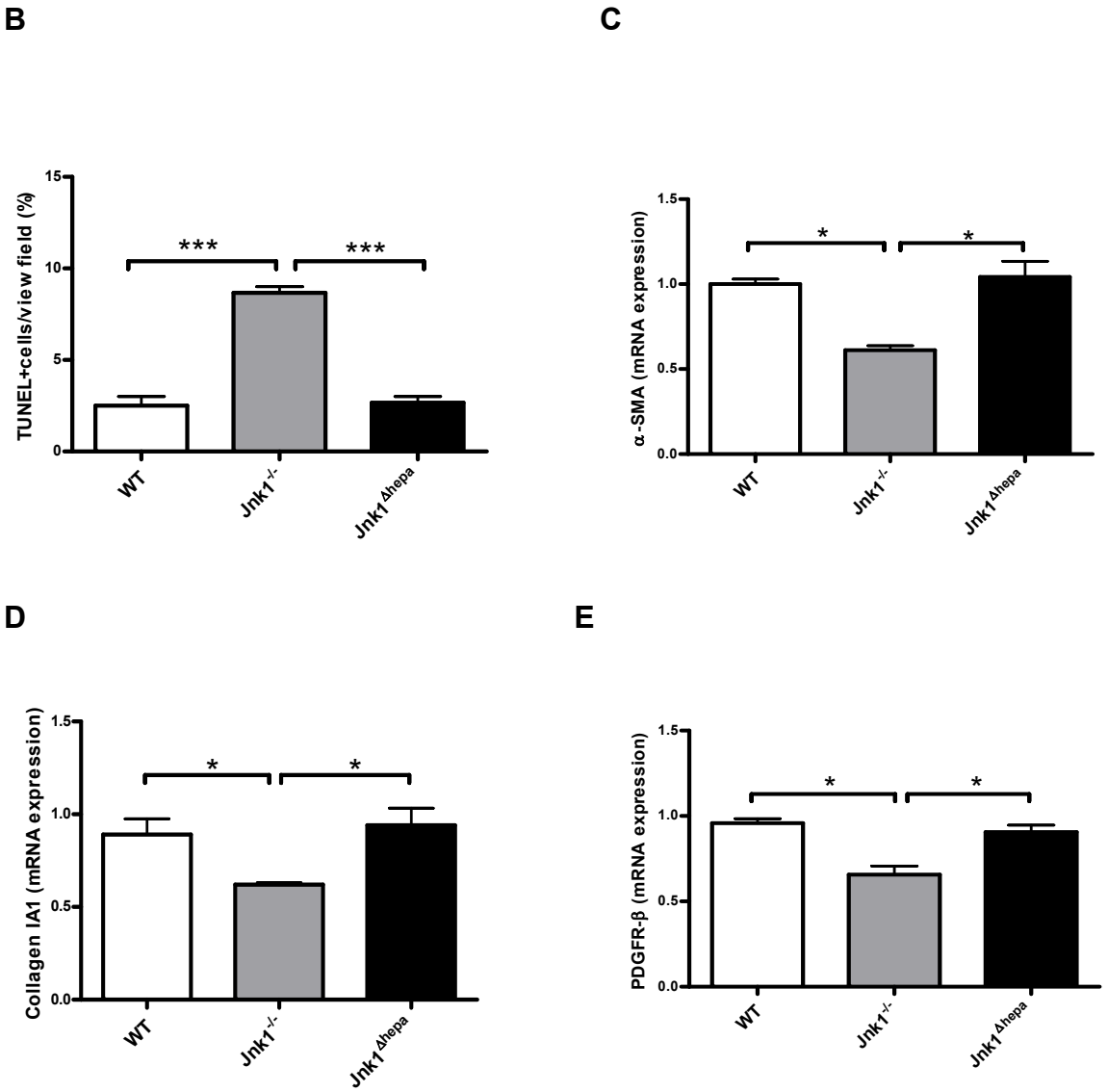

Figure 23. Lack of JNK1 expression in HSCs triggers HSC apoptosis and reduces transdifferentiation. (A) Representative TUNEL staining of primary HSCs from WT, Jnk1$^{-/-}$ and Jnk1$^{\Delta hepa}$ mice at day 7 of culture, and quantification of positive cells **(B)**. **(C-E)** mRNA expression analysis of Collagen IA1 **(C)**, PDGFR-β **(D)** and α-SMA **(E)** was quantified by RT-PCR of samples taken from isolated primary HSCs after 7 days in culture. Values are mean ± SEM from at least 7 mice per group (*p<0.05, ***p<0.001).

4. Discussion

JNK are members of the MAPK family involved in the regulation of cell death, proliferation, metabolism and inflammation[80]. JNK1 and JNK2 are both expressed in the liver. At present it is not well defined if these two genes have synergistic or antagonistic functions during the progression of acute and chronic liver diseases. One of the tasks to truly understand the role of JNK for liver physiology and pathophysiology is to characterize and identify their cell-type specific function under different conditions. Parenchymal and NPCs as well as immune infiltrating cells contribute to mechanisms of liver injury and repair. In this context, cell-type specific activation of JNK family members might be relevant to determine the outcome of liver disease.

In the present study we were interested in defining the relevance of JNK1 activation in different liver cell compartments during liver fibrosis. We used two widely accepted *in vivo* experimental models of liver fibrosis[81-82]; (i) the surgical BDL-model of biliary fibrosis and (ii) the pharmacological CCl_4 model of globular fibrosis. For this approach we generated hepatocyte-specific JNK1 knockout mice. JNK1 complete knockout mice as well as the respective controls were included. Moreover, we performed BMT to investigate the relevance of JNK1 activation in bone marrow-derived cells and investigated the contribution of JNK1 *in vivo* and *in vitro* in HSCs to define their function during liver fibrogenesis. Interestingly, our results demonstrated that JNK1 activation in HSCs plays an essential role during their transdifferentiation and thus we define JNK1 in HSCs as a profibrogenic mediator since deletion of JNK1 reduces liver fibrogenesis.

4.1 The contribution of JNK1 in hepatocytes and NPCs to chronic liver injury

Earlier studies have examined the relevance of JNK activation not only in acute but also in chronic liver injury[83]. Especially JNK1 has been reported to play a crucial role in response to TNF[84], Concanavalin A[85], ischemia-reperfusion[64, 80] acetaminophen intoxication[86], HFD[87] and hepatic carcinogens[88]. Therefore, we first investigated the role of hepatocyte-specific JNK1 during chronic liver injury in the CCl_4 and BDL model of liver fibrosis. The results show fellow as: Firstly,

macroscopical examination of 28 days-BDL-subjected liver specimens of WT and Jnk1$^{\Delta hepa}$ mice revealed no different of the presence of necrotic foci in distinct hepatic lobes. H&E staining of WT and Jnk1$^{\Delta hepa}$ livers also showed no differences concerning cholestatic hepatitis with widespread bile infarcts. In contrast, Jnk1$^{-/-}$ mice exhibited signs of ductular proliferation but no necrotic foci. Biliary infarcts in Jnk1$^{-/-}$ mice compared with WT and Jnk1$^{\Delta hepa}$ 4 weeks after BDL were dramatically reduced. For mice treated with CCl_4, H&E staining of Jnk1$^{\Delta hepa}$ and WT livers revealed more cellular damage and centrilobular congestion of inflammatory cells compared to Jnk1$^{-/-}$ mice, while WT and Jnk1$^{\Delta hepa}$ liver have the same phenotype. Plasma AST and ALT levels increased at same folds in Jnk1$^{\Delta hepa}$ and WT compared with respective sham-operated animals. Moreover, Bile duct ligated Jnk1$^{\Delta hepa}$ and WT mice exhibited significantly more hyperbilirubinemia and AP compared with Jnk1$^{-/-}$ mice, but we did not find significant differences when WT and Jnk1$^{\Delta hepa}$ mice were compared. TUNEL staining shows Jnk1$^{-/-}$ animals showed significantly less TUNEL-positive cells than WT and Jnk1$^{\Delta hepa}$ mice 28 days after CCl_4 and BDL treatment. However, WT and Jnk1$^{\Delta hepa}$ mice showed no difference. In summary, these data indicate that JNK1 expression in hepatocytes has no impact on hepatocellular injury in two different models of chronic experimental liver injury, which means that JNK1 in hepatocytes had no major impact on the progression of liver disease.

However, the role of JNK in apoptosis remains highly controversial[89-91]. Some authors suggested a pro-apoptotic role of JNK1 during TNF-induced apoptosis *in vitro*[63] and *in vivo*[64]. Under normal circumstances, transient JNK activation confers cytoprotection[92-93]. However, our preliminary results (Cubero *et al*, unpublished) suggest that NF-κB has a major impact on the role of JNK1 during chronic liver injury. Deletion of the IKK regulatory subunit IKKγ/NEMO blocks NF-κB activation. As a consequence, the NF-kB-dependent anti-oxidative response is severely impaired, triggering prolonged JNK1 activation and resulting in increased apoptosis (Cubero *et al*, unpublished results).

4.2 The role of JNK1 in hepatocytes and NPCs to liver fibrosis

In our experiments we found that repeated CCl_4 injections and BDL induced severe collagen deposition and septum formation in Jnk1$^{\Delta hepa}$ and WT livers,

classified by Sirius Red staining. In contrast, quantification of Sirius Red staining revealed significantly lower collagen fibre formation in Jnk1$^{-/-}$ livers. These findings were further validated by measuring α-SMA and Collagen IA1 mRNA and protein expression. Jnk1$^{-/-}$ livers show reduced α-SMA and Collagen IA1 expression compared with Jnk1$^{\Delta hepa}$ and WT animals, in both experimental models.

Several reports have supported the hypothesis that JNK1 is necessary for the development of fibrosis in organs such as lung and kidney[94-95]. Indeed, Kluwe and collaborators[59] had previously reported that genetic deletion of JNK1 or its pharmacological inhibition by SP600125 did not improve hepatocellular injury as measured by transaminase levels or changes in bile infarcts in the CCl_4 and BDL-model up to three weeks. In line with these results, we observed no difference during the early phase of liver injury in both experimental models using Jnk1$^{-/-}$, Jnk1$^{\Delta hepa}$ or WT animals (data not shown). However, liver injury was significantly reduced in Jnk1$^{-/-}$ animals after 4 weeks of CCl_4 or BDL treatment. A possible explanation for these differences is the duration of chronic injury since prolonged liver damage results in stronger fibrosis and consequently in liver cirrhosis[96] which might be also secondary to the observed effect of impaired HSCs transdifferentiation in Jnk1$^{-/-}$ animals.

In Jnk1$^{-/-}$ livers reduced hepatocyte proliferation was observed in both experimental models of liver injury compared with Jnk1$^{\Delta hepa}$ or WT animals. Since Jnk1$^{-/-}$ animals also showed reduced liver injury, it is likely that this observation is rather a consequence than a primary JNK1-dependent effect. The role of JNK1 during liver regeneration has been investigated. Recent studies[88, 97] suggest a cell-specific and crucial role of JNK in liver regeneration. In accordance with the study by Das[97], our data would strengthen the finding that JNK1 activation during the regenerative response is not important in liver parenchymal cells but in other cells which contribute to the proliferative response of hepatocytes. PCNA, Cyclin D and Cyclin A levels on the mRNA and protein lever were strongly up-regulated in Jnk1$^{\Delta hepa}$ and WT livers 4 weeks after BDL or after repetitive CCl_4 treatment, respectively. In contrast, these changes were significantly less severe in Jnk1$^{-/-}$ mice suggesting reduced compensatory proliferation after injury in both experimental models. Moreover, quantification of cell proliferation with Ki-67 immunostaining demonstrated lower proliferation rates in Jnk1$^{-/-}$ compared with Jnk1$^{\Delta hepa}$ and WT

livers treated with CCl_4 or with BDL for 4 weeks. Interestingly, WT and Jnk1$^{\Delta hepa}$ mice showed the same rate of hepatocyte proliferation.

4.3 The analysis of the function of JNK1 in BM-derived cells during liver injury

As the experiments using Jnk1$^{\Delta hepa}$ mice clearly demonstrated that JNK1 in hepatocytes has no impact on the progression of liver fibrosis in both models of injury, we next investigated the contribution of BM-derived cells. Previous studies revealed that JNK1 activation in e.g. KCs is relevant during hepatic inflammation and thus in the end might contribute to liver fibrosis[98-99]. Additionally, KCs can interact with HSCs, accelerate their activation, and promote their fibrogenic responses *in vitro*[99]. To this end, lethally irradiated WT or Jnk1$^{-/-}$ mice were reconstituted with bone marrow from WT or Jnk1$^{-/-}$ donors and treated with antibiotics to reduce postoperative infection and inflammation.

In our experiments, KCs recovery was ensured since we performed CCl_4 or BDL 5 weeks after the injection of BM-derived cells. Unexpectedly, our results showed that JNK1 in BM-derived cells does not significantly contribute to liver fibrosis. These results were further confirmed by transplanting WT or Jnk1$^{-/-}$ BM into Jnk1$^{\Delta hepa}$ animals. Evidence is as follows: Firstly, the BDL treated chimeric WT mice reconstituted with WT (WT→WT) and Jnk1$^{-/-}$ BM (Jnk1$^{-/-}$→WT) showed macroscopically yellowish dots and necrotic foci in HE staining while Jnk1$^{-/-}$ recipients transplanted with either WT or Jnk1$^{-/-}$ BM (WT/Jnk1$^{-/-}$→Jnk1$^{-/-}$) showed no external signs of liver injury. Secondly , Along with the first results, plasma AST, ALT, Bilirubin and AP levels evidenced significantly higher liver damage after BDL in WT mice reconstituted with WT BM (WT→WT) or Jnk1$^{-/-}$ BM (Jnk1$^{-/-}$→WT). Thirdly, in both fibrosis model, WT animals reconstituted with WT or Jnk1$^{-/-}$ BM showed more matrix deposition compared with Jnk1$^{-/-}$ mice reconstituted with Jnk1$^{-/-}$ or WT BM by Sirius red staining and Collagen IA1 immunostaining in the livers.

These experiments showed no significant differences in liver fibrogenesis in hepatocyte-specific JNK1 knockout animals reconstituted with WT or Jnk1$^{-/-}$ BM-derived cells (data not shown).

4.4 Assess the role of JNK1 in HSCs *in vivo* and *in vitro*

The knockout and BM experiments strongly suggested that NPCs are essential in mediating the JNK1-dependent pro-fibrogenic effect during chronic liver injury. Among NPCs, cholangiocytes, non-bone marrow-derived KC, endothelial cells or HSCs could be responsible for mediating the JNK1-dependent effect on liver fibrosis. Therefore, at this point, we followed two different strategies to identify precisely the NPCs important in mediating this effect. We included array analysis and immunohistochemistry studies, performed by an experienced pathologist, 4 weeks after chronic liver injury. Microarray analysis suggested HSCs-marker genes *raet1d*, or genes associated with hepatic fibrosis such as *mmd2*, *gas1*, and *grem1*, *timp4* (or *mmp7* were differentially clustered according to fold change. These genes were down-regulated in Jnk1$^{-/-}$ compared with WT and Jnk1$^{\Delta hepa}$ livers. Moreover, genes related to protection against fibrosis such as *saa1* or *saa2* were highly up-regulated in Jnk1$^{-/-}$ and strongly down-regulated in Jnk1$^{\Delta hepa}$ mice. Immunohistochemistry staining showed that α-SMA positive activated HSCs in Jnk1$^{-/-}$ mice were less in number compared to WT and Jnk1$^{\Delta hepa}$ mice and that the septa are more slender. Both independent analyses pointed at the HSC compartment as the cell population involved in mediating the JNK1-dependent pro-fibrogenic effect on liver fibrogenesis.

To test the relevance of our *in vivo* observation we isolated primary HSCs from WT, Jnk1$^{\Delta hepa}$ and Jnk1$^{-/-}$ mice. Here, we used a recently established novel cell sorting technique developed in our Department which provides high HSC purity[5]. The 'conventional' HSCs isolation using the diverse density gradient methods has for a long time remained the 'gold standard' method, mainly due to the fact that it allows for isolating fairly large numbers of HSCs with acceptable purity[100]. However, conventional HSC purification protocols result in a purity of only approximately 75% HSCs[100]. Due to these challenges, our team has established protocols to isolate HSCs by FACS. HSCs from mice were purified by cell sorting using simply their high side scatter of incident light[101]. Starting from crude cell fractions that were 50–70% enriched by conventional density centrifugation, the obtained cell purity after sorting (in which 1.4 ± 0.4 million cells were sorted per hour) was found to be over 96% and the viability of resulting cells was approximately 90%, as measured by Trypan blue exclusion testing .

HSCs from WT, Jnk1$^{\Delta hepa}$ and Jnk1$^{-/-}$ were cultured for up to 10 days. These results visibly strengthened the *in vivo* findings and demonstrated that JNK1 is crucial in the early stages of normal HSCs activation as well as in later phases when these cells express α-SMA. Our data show that the lower profibrogenic response of Jnk1$^{-/-}$ mice is due to the poor rate of proliferation and survival of Jnk1$^{-/-}$ HSCs associated with decreased expression of α-SMA, Collagen IA1 and PDGFR-β. Moreover, apoptosis of Jnk1$^{-/-}$ HSCs helps to prevent the fibrogenic cascade, a phenomenon also observed in C/EBP-β deleted mice[102].

We used a knockout for JNK1 in hepatocytes to specifically define the role of cell-type JNK1 in liver fibrogenesis. Here, we report for the first time that JNK1 in hepatocytes is not important for the development of liver fibrosis. Additionally, the BMT experiments strongly argue against the hypothesis that JNK1 knockout in bone marrow-derived cells have an effect on hepatic fibrosis. Finally, our data point at JNK1 as an essential pro-fibrogenic kinase in HSCs and portal myfibroblasts for the pathogenesis of different types of liver fibrosis (biliary and hepatocytic). Altogether, our results shed new light and contribute to previous findings[59] in the yet undefined field of liver fibrosis and activation of the MAPK signalling pathway. In summary, our results suggest that cell-type specific inhibition of JNK1 in HSCs might be an attractive therapeutic approach for treating liver fibrosis, thus opening a new door for the treatment of patients.

5. Summary

Liver fibrosis is the body's response to persistant hepatic injury, which frequently triggers liver cirrhosis and HCC. JNKs are activated in response to stimuli such as inflammatory cytokines, bacterial products, oxidative stress, toxins, drugs, and metabolic changes. Indeed, JNK contribute to ECM deposition during myofibroblast differentiation suggesting a potential role for the JNK genes in liver fibrogenesis. However, the specific role of the JNK genes, and specifically of JNK1, during liver fibrosis remains elusive.

The present study aimed to investigate target cell types and molecular mechanisms involved in mediating JNK1-dependent effects. WT, $Jnk1^{-/-}$ and $Jnk1^{\Delta hepa}$ mice were subjected to BDL or chronic CCl_4 treatment. Additionally, the contribution of bone-marrow derived cells and HSC was investigated. Serum markers of liver damage (liver transaminases, AP and bilirubin) and liver histology revealed reduced injury in $Jnk1^{-/-}$ compared to WT and $Jnk1^{\Delta hepa}$ mice. Hepatocyte cell death and proliferation was reduced in $Jnk1^{-/-}$ compared to WT and $Jnk1^{\Delta hepa}$ livers. Parameters of liver fibrosis such as Sirius Red staining as well as Collagen IA1 and α-SMA expression were down-regulated in $Jnk1^{-/-}$ compared to WT and $Jnk1^{\Delta hepa}$ livers, 4 weeks after CCl_4 or BDL. BMT experiments excluded bone marrow derived cells from having a major impact on the JNK1-dependent effect on fibrogenesis. Primary HSCs from $Jnk1^{-/-}$ livers showed reduced transdifferentiation compared with WT and $Jnk1^{\Delta hepa}$-derived HSCs.

We report for the first time that JNK1 in hepatocytes is not important for the development of liver fibrosis. Additionally, the BMT experiments strongly argue against the hypothesis that JNK1 knockout in bone marrow-derived cells have an effect on hepatic fibrosis. Finally, our data point at JNK1 as an essential pro-fibrogenic kinase in HSCs and portal myfibroblasts for the pathogenesis of different types of liver fibrosis (biliary and hepatocytic). In the future cell-type specific inhibition of JNK1 in HSCs might be an attractive therapeutic approach for treating liver fibrosis, thus opening a new door for the treatment of patients.

6. Zusammenfassung

Leberfibrose resultiert aus einer chronischen Leberschädigung, die sich im Verlauf zur Leberzirrhose bis hin zum hepatozellulären Karzinom (HCC) entwickeln kann. Die Jun-Kinasen (JNK) werden durch unterschiedliche Stimuli, wie Zytokine, bakterielle Mediatoren, oxidativen Stress, Toxine oder bestimmte Stoffwechselprodukte aktiviert. Sie sind wichtig für den Aufbau der extrazellulären Matrix im Rahmen der Reifung von Myofibroblasten, weshalb den JNK eine entscheidende Bedeutung bei der Entstehung der Leberfibrose zukommen kann. Die zugrundeliegenden Mechanismen und insbesondere die Funktionen der JNK-Isoformen für die Fibroseentstehung, insbesondere von JNK1, sind bisher unklar.

Ziel dieser Arbeit war es, die molekularen Mechanismen und die zelltyp-spezifische Bedeutung von JNK1 für die Leberfibroseentstehung zu charakterisieren. An Wildtypmäusen (WT), konstitutiven JNK1 Knockoutmäusen ($Jnk1^{-/-}$) und hepatozytenspezifischen Knockoutmäusen ($Jnk1^{\Delta hepa}$) wurden zwei etablierte Modelle der Fibroseentstehung in der Leber untersucht. Dies sind die Gallengangsligatur (BDL) und die chronische Leberschädigung durch CCl_4, weiterhin erfolgten Knochenmarkstransplantationen und in vitro Experimente mit HSCs. Serummarker für Leberschädigung wie Transaminasen, alkalische Phosphatase und Biliurubin sowie die histologische Aufarbeitung zeigten eine verminderte Leberschädigung in $Jnk1^{-/-}$ im Vergleich zu WT and $Jnk1^{\Delta hepa}$ Mäusen. Sowohl die Apoptose- als auch die Zellproliferation von Hepatozyten waren vermindert in $Jnk1^{-/-}$ im Vergleich zu WT and $Jnk1^{\Delta hepa}$ Lebern. Die Leberfibrose, quantifiziert anhand von Sirius Red Färbungen, Messungen der Collagen IA1 und α-SMA Expression war weniger ausgeprägt in $Jnk1^{-/-}$ im Vergleich zu WT und $Jnk1^{\Delta hepa}$ Lebern 4 Wochen nach CCl_4 oder BDL. Durch die Ergebnisse der BMT Experimente konnte ein wesentlicher Effekt von Zellen der myeloischen Reihe bei der JNK1-abhängigen Leberfibrose ausgeschlossen werden. Weiterführende Experimente ergaben, dass insbesondere die JNK1-Expression in HSCs eine wesentliche Rolle für die Fibroseentstehung spielt.

Durch diese Arbeit wurde erstmalig gezeigt, dass JNK1 in Hepatozyten keine entscheidende Rolle bei der Fibroseentstehung spielt. Zusätzlich sprechen die Ergebnisse der BMT Experimente gegen einen relevanten Effekt von JNK1 in Zellen

der myeloischen Reihe. Die Daten deuten auf eine substantielle Rolle von JNK1 als profibrotische Proteinkinase in HSCs und portalen Myofibroblasten hin. In Zukunft könnte eine HSCs-spezifische Modulation der JNK1 Aktivität als therapeutischer Ansatz bei Patienten mit Leberfibrose und Zirrhose in Frage kommen.

7. References:

1. Tobkes AI, Nord HJ. Liver biopsy: review of methodology and complications. Dig Dis 1995;13:267-74.
2. Sasse D, Spornitz UM, Maly IP. Liver architecture. Enzyme 1992;46:8-32.
3. Motta PM. The three-dimensional microanatomy of the liver. Arch Histol Jpn 1984;47:1-30.
4. Liaskou E, Wilson DV, Oo YH. Innate immune cells in liver inflammation. Mediators Inflamm 2012;2012:949157.
5. Tacke F, Weiskirchen R. Update on hepatic stellate cells: pathogenic role in liver fibrosis and novel isolation techniques. Expert Rev Gastroenterol Hepatol 2012;6:67-80.
6. Fausto N. Liver regeneration and repair: hepatocytes, progenitor cells, and stem cells. Hepatology 2004;39:1477-87.
7. Taub R. Liver regeneration: from myth to mechanism. Nat Rev Mol Cell Biol 2004;5:836-47.
8. Friedman SL. Liver fibrosis -- from bench to bedside. J Hepatol 2003;38 Suppl 1:S38-53.
9. Bataller R, Brenner DA. Liver fibrosis. J Clin Invest 2005;115:209-18.
10. Gines P, Cardenas A, Arroyo V, et al. Management of cirrhosis and ascites. N Engl J Med 2004;350:1646-54.
11. Pinzani M. Liver fibrosis. Springer Semin Immunopathol 1999;21:475-90.
12. Benyon RC, Iredale JP. Is liver fibrosis reversible? Gut 2000;46:443-6.
13. Arthur MJ. Fibrogenesis II. Metalloproteinases and their inhibitors in liver fibrosis. Am J Physiol Gastrointest Liver Physiol 2000;279:G245-9.
14. Bataller R, North KE, Brenner DA. Genetic polymorphisms and the progression of liver fibrosis: a critical appraisal. Hepatology 2003;37:493-503.
15. Takehara T, Tatsumi T, Suzuki T, et al. Hepatocyte-specific disruption of Bcl-xL leads to continuous hepatocyte apoptosis and liver fibrotic responses. Gastroenterology 2004;127:1189-97.
16. Canbay A, Higuchi H, Bronk SF, et al. Fas enhances fibrogenesis in the bile duct ligated mouse: a link between apoptosis and fibrosis. Gastroenterology 2002;123:1323-30.
17. Safadi R, Ohta M, Alvarez CE, et al. Immune stimulation of hepatic fibrogenesis by CD8 cells and attenuation by transgenic interleukin-10 from hepatocytes. Gastroenterology 2004;127:870-82.
18. Yoshida T, Ogata H, Kamio M, et al. SOCS1 is a suppressor of liver fibrosis and hepatitis-induced carcinogenesis. J Exp Med 2004;199:1701-7.
19. Sahai A, Malladi P, Melin-Aldana H, et al. Upregulation of osteopontin expression is involved in the development of nonalcoholic steatohepatitis in a dietary murine model. Am J Physiol Gastrointest Liver Physiol 2004;287:G264-73.
20. Ueberham E, Low R, Ueberham U, et al. Conditional tetracycline-regulated expression of TGF-beta1 in liver of transgenic mice leads to reversible intermediary fibrosis. Hepatology 2003;37:1067-78.
21. Yoshiji H, Kuriyama S, Yoshii J, et al. Tissue inhibitor of metalloproteinases-1 attenuates spontaneous liver fibrosis resolution in the transgenic mouse. Hepatology 2002;36:850-60.
22. Hepatic stellate cell nomenclature. Hepatology 1996;23:193.

23. Rockey DC. Hepatic blood flow regulation by stellate cells in normal and injured liver. Semin Liver Dis 2001;21:337-49.
24. Friedman SL. Hepatic stellate cells: protean, multifunctional, and enigmatic cells of the liver. Physiol Rev 2008;88:125-72.
25. Rippe RA, Brenner DA. From quiescence to activation: Gene regulation in hepatic stellate cells. Gastroenterology 2004;127:1260-2.
26. Bachem MG, Meyer D, Melchior R, et al. Activation of rat liver perisinusoidal lipocytes by transforming growth factors derived from myofibroblastlike cells. A potential mechanism of self perpetuation in liver fibrogenesis. J Clin Invest 1992;89:19-27.
27. Parola M, Pinzani M, Casini A, et al. Stimulation of lipid peroxidation or 4-hydroxynonenal treatment increases procollagen alpha 1 (I) gene expression in human liver fat-storing cells. Biochem Biophys Res Commun 1993;194:1044-50.
28. Friedman SL. Mechanisms of hepatic fibrogenesis. Gastroenterology 2008;134:1655-69.
29. Purps O, Lahme B, Gressner AM, et al. Loss of TGF-beta dependent growth control during HSC transdifferentiation. Biochem Biophys Res Commun 2007;353:841-7.
30. Senoo H, Yoshikawa K, Morii M, et al. Hepatic stellate cell (vitamin A-storing cell) and its relative--past, present and future. Cell Biol Int;34:1247-72.
31. Hernandez-Gea V, Friedman SL. Pathogenesis of liver fibrosis. Annu Rev Pathol;6:425-56.
32. Seki E, De Minicis S, Osterreicher CH, et al. TLR4 enhances TGF-beta signaling and hepatic fibrosis. Nat Med 2007;13:1324-32.
33. Karlmark KR, Weiskirchen R, Zimmermann HW, et al. Hepatic recruitment of the inflammatory Gr1+ monocyte subset upon liver injury promotes hepatic fibrosis. Hepatology 2009;50:261-74.
34. Friedman SL. Evolving challenges in hepatic fibrosis. Nat Rev Gastroenterol Hepatol;7:425-36.
35. Iredale JP. Models of liver fibrosis: exploring the dynamic nature of inflammation and repair in a solid organ. J Clin Invest 2007;117:539-48.
36. Novo E, di Bonzo LV, Cannito S, et al. Hepatic myofibroblasts: a heterogeneous population of multifunctional cells in liver fibrogenesis. Int J Biochem Cell Biol 2009;41:2089-93.
37. Jhandier MN, Kruglov EA, Lavoie EG, et al. Portal fibroblasts regulate the proliferation of bile duct epithelia via expression of NTPDase2. J Biol Chem 2005;280:22986-92.
38. Kallis YN, Forbes SJ. The bone marrow and liver fibrosis: friend or foe? Gastroenterology 2009;137:1218-21.
39. Zeisberg M, Yang C, Martino M, et al. Fibroblasts derive from hepatocytes in liver fibrosis via epithelial to mesenchymal transition. J Biol Chem 2007;282:23337-47.
40. Wells RG. The epithelial-to-mesenchymal transition in liver fibrosis: here today, gone tomorrow? Hepatology;51:737-40.
41. Popov Y, Schuppan D. Epithelial-to-mesenchymal transition in liver fibrosis: dead or alive? Gastroenterology;139:722-5.
42. Arthur MJ. Reversibility of liver fibrosis and cirrhosis following treatment for hepatitis C. Gastroenterology 2002;122:1525-8.

43. Firpi RJ, Nelson DR. Viral hepatitis: manifestations and management strategy. Hematology Am Soc Hematol Educ Program 2006:375-80.
44. Tome S, Lucey MR. Review article: current management of alcoholic liver disease. Aliment Pharmacol Ther 2004;19:707-14.
45. Baroni GS, D'Ambrosio L, Curto P, et al. Interferon gamma decreases hepatic stellate cell activation and extracellular matrix deposition in rat liver fibrosis. Hepatology 1996;23:1189-99.
46. Neuschwander-Tetri BA, Brunt EM, Wehmeier KR, et al. Improved nonalcoholic steatohepatitis after 48 weeks of treatment with the PPAR-gamma ligand rosiglitazone. Hepatology 2003;38:1008-17.
47. Tomita K, Azuma T, Kitamura N, et al. Pioglitazone prevents alcohol-induced fatty liver in rats through up-regulation of c-Met. Gastroenterology 2004;126:873-85.
48. Iimuro Y, Gallucci RM, Luster MI, et al. Antibodies to tumor necrosis factor alfa attenuate hepatic necrosis and inflammation caused by chronic exposure to ethanol in the rat. Hepatology 1997;26:1530-7.
49. Fang B, Shi M, Liao L, et al. Systemic infusion of FLK1(+) mesenchymal stem cells ameliorate carbon tetrachloride-induced liver fibrosis in mice. Transplantation 2004;78:83-8.
50. Kollet O, Shivtiel S, Chen YQ, et al. HGF, SDF-1, and MMP-9 are involved in stress-induced human CD34+ stem cell recruitment to the liver. J Clin Invest 2003;112:160-9.
51. Wagner EF, Nebreda AR. Signal integration by JNK and p38 MAPK pathways in cancer development. Nat Rev Cancer 2009;9:537-49.
52. Seki E, Brenner DA, Karin M. A liver full of JNK: signaling in regulation of cell function and disease pathogenesis, and clinical approaches. Gastroenterology 2012;143:307-20.
53. Bogoyevitch MA, Ngoei KR, Zhao TT, et al. c-Jun N-terminal kinase (JNK) signaling: recent advances and challenges. Biochim Biophys Acta;1804:463-75.
54. Haeusgen W, Herdegen T, Waetzig V. The bottleneck of JNK signaling: molecular and functional characteristics of MKK4 and MKK7. Eur J Cell Biol;90:536-44.
55. Liu J, Lin A. Role of JNK activation in apoptosis: a double-edged sword. Cell Res 2005;15:36-42.
56. Lin A. A five-year itch in TNF-alpha cytotoxicity: the time factor determines JNK action. Dev Cell 2006;10:277-8.
57. Behrens A, Sibilia M, David JP, et al. Impaired postnatal hepatocyte proliferation and liver regeneration in mice lacking c-jun in the liver. EMBO J 2002;21:1782-90.
58. Stepniak E, Ricci R, Eferl R, et al. c-Jun/AP-1 controls liver regeneration by repressing p53/p21 and p38 MAPK activity. Genes Dev 2006;20:2306-14.
59. Kluwe J, Pradere JP, Gwak GY, et al. Modulation of hepatic fibrosis by c-Jun-N-terminal kinase inhibition. Gastroenterology 2010;138:347-59.
60. Ventura JJ, Cogswell P, Flavell RA, et al. JNK potentiates TNF-stimulated necrosis by increasing the production of cytotoxic reactive oxygen species. Genes Dev 2004;18:2905-15.
61. Weiss L, Whitmarsh AJ, Yang DD, et al. Regulation of c-Jun NH(2)-terminal kinase (Jnk) gene expression during T cell activation. J Exp Med 2000;191:139-46.

62. Chen N, She QB, Bode AM, et al. Differential gene expression profiles of Jnk1- and Jnk2-deficient murine fibroblast cells. Cancer Res 2002;62:1300-4.
63. Liu X, Kim CN, Yang J, et al. Induction of apoptotic program in cell-free extracts: requirement for dATP and cytochrome c. Cell 1996;86:147-57.
64. Chang L, Kamata H, Solinas G, et al. The E3 ubiquitin ligase itch couples JNK activation to TNFalpha-induced cell death by inducing c-FLIP(L) turnover. Cell 2006;124:601-13.
65. Wang Y, Singh R, Lefkowitch JH, et al. Tumor necrosis factor-induced toxic liver injury results from JNK2-dependent activation of caspase-8 and the mitochondrial death pathway. J Biol Chem 2006;281:15258-67.
66. Liedtke C, Trautwein C. The role of JNK2 in toxic liver injury. J Hepatol 2006;45:762-4.
67. Hatting M, Trautwein C, Cubero FJ. TAL deficiency, all roads lead to oxidative stress? Hepatology 2009;50:979-81.
68. Cubero FJ, Drvarov O, Trautwein C. c-Jun NH(2)-terminal kinase 1 in hepatocytes: an essential mediator of insulin resistance. Hepatology 2010;51:2221-3.
69. Schattenberg JM, Wang Y, Singh R, et al. Hepatocyte CYP2E1 overexpression and steatohepatitis lead to impaired hepatic insulin signaling. J Biol Chem 2005;280:9887-94.
70. Schattenberg JM, Singh R, Wang Y, et al. JNK1 but not JNK2 promotes the development of steatohepatitis in mice. Hepatology 2006;43:163-72.
71. Hirosumi J, Tuncman G, Chang L, et al. A central role for JNK in obesity and insulin resistance. Nature 2002;420:333-6.
72. Tuncman G, Hirosumi J, Solinas G, et al. Functional in vivo interactions between JNK1 and JNK2 isoforms in obesity and insulin resistance. Proc Natl Acad Sci U S A 2006;103:10741-6.
73. Chen F, Beezhold K, Castranova V. JNK1, a potential therapeutic target for hepatocellular carcinoma. Biochim Biophys Acta 2009;1796:242-51.
74. Schnabl B, Bradham CA, Bennett BL, et al. TAK1/JNK and p38 have opposite effects on rat hepatic stellate cells. Hepatology 2001;34:953-63.
75. Gentleman RC, Carey VJ, Bates DM, et al. Bioconductor: open software development for computational biology and bioinformatics. Genome Biol 2004;5:R80.
76. Takagi M, Fukui Y, Wakitani S, et al. Effect of poly DL-lactic-co-glycolic acid mesh on a three-dimensional culture of chondrocytes. J Biosci Bioeng 2004;98:477-81.
77. Pfaffl MW. A new mathematical model for relative quantification in real-time RT-PCR. Nucleic Acids Res 2001;29:e45.
78. Bradford MM. A rapid and sensitive method for the quantitation of microgram quantities of protein utilizing the principle of protein-dye binding. Anal Biochem 1976;72:248-54.
79. Louis H, Van Laethem JL, Wu W, et al. Interleukin-10 controls neutrophilic infiltration, hepatocyte proliferation, and liver fibrosis induced by carbon tetrachloride in mice. Hepatology 1998;28:1607-15.
80. Weston CR, Davis RJ. The JNK signal transduction pathway. Curr Opin Genet Dev 2002;12:14-21.
81. Tsukamoto H, Matsuoka M, French SW. Experimental models of hepatic fibrosis: a review. Semin Liver Dis 1990;10:56-65.

82. Constandinou C, Henderson N, Iredale JP. Modeling liver fibrosis in rodents. Methods Mol Med 2005;117:237-50.
83. Das M, Sabio G, Jiang F, et al. Induction of hepatitis by JNK-mediated expression of TNF-alpha. Cell 2009;136:249-60.
84. Schwabe RF, Brenner DA. Mechanisms of Liver Injury. I. TNF-alpha-induced liver injury: role of IKK, JNK, and ROS pathways. Am J Physiol Gastrointest Liver Physiol 2006;290:G583-9.
85. Ni HM, Chen X, Ding WX, et al. Differential roles of JNK in ConA/GalN and ConA-induced liver injury in mice. Am J Pathol 2008;173:962-72.
86. An J, Mehrhof F, Harms C, et al. ARC is a novel therapeutic approach against acetaminophen-induced hepatocellular necrosis. J Hepatol 2012.
87. Sabio G, Cavanagh-Kyros J, Ko HJ, et al. Prevention of steatosis by hepatic JNK1. Cell Metab 2009;10:491-8.
88. Hui L, Zatloukal K, Scheuch H, et al. Proliferation of human HCC cells and chemically induced mouse liver cancers requires JNK1-dependent p21 downregulation. J Clin Invest 2008;118:3943-53.
89. De Smaele E, Zazzeroni F, Papa S, et al. Induction of gadd45beta by NF-kappaB downregulates pro-apoptotic JNK signalling. Nature 2001;414:308-13.
90. Natoli G, Costanzo A, Ianni A, et al. Activation of SAPK/JNK by TNF receptor 1 through a noncytotoxic TRAF2-dependent pathway. Science 1997;275:200-3.
91. Tang G, Minemoto Y, Dibling B, et al. Inhibition of JNK activation through NF-kappaB target genes. Nature 2001;414:313-7.
92. Wicovsky A, Muller N, Daryab N, et al. Sustained JNK activation in response to tumor necrosis factor is mediated by caspases in a cell type-specific manner. J Biol Chem 2007;282:2174-83.
93. Krause D, Lyons A, Fennelly C, et al. Transient activation of Jun N-terminal kinases and protection from apoptosis by the insulin-like growth factor I receptor can be suppressed by dicumarol. J Biol Chem 2001;276:19244-52.
94. Alcorn JF, van der Velden J, Brown AL, et al. c-Jun N-terminal kinase 1 is required for the development of pulmonary fibrosis. Am J Respir Cell Mol Biol 2009;40:422-32.
95. Ma FY, Flanc RS, Tesch GH, et al. A pathogenic role for c-Jun amino-terminal kinase signaling in renal fibrosis and tubular cell apoptosis. J Am Soc Nephrol 2007;18:472-84.
96. Fujii T, Fuchs BC, Yamada S, et al. Mouse model of carbon tetrachloride induced liver fibrosis: Histopathological changes and expression of CD133 and epidermal growth factor. BMC Gastroenterol 2010;10:79.
97. Das M, Garlick DS, Greiner DL, et al. The role of JNK in the development of hepatocellular carcinoma. Genes Dev 2011;25:634-45.
98. Solinas G, Vilcu C, Neels JG, et al. JNK1 in hematopoietically derived cells contributes to diet-induced inflammation and insulin resistance without affecting obesity. Cell Metab 2007;6:386-97.
99. Kodama Y, Kisseleva T, Iwaisako K, et al. c-Jun N-terminal kinase-1 from hematopoietic cells mediates progression from hepatic steatosis to steatohepatitis and fibrosis in mice. Gastroenterology 2009;137:1467-1477 e5.
100. Weiskirchen R, Gressner AM. Isolation and culture of hepatic stellate cells. Methods Mol Med 2005;117:99-113.
101. Geerts A, Niki T, Hellemans K, et al. Purification of rat hepatic stellate cells by side scatter-activated cell sorting. Hepatology 1998;27:590-8.

102. Amali AA, Rekha RD, Lin CJ, et al. Thioacetamide induced liver damage in zebrafish embryo as a disease model for steatohepatitis. J Biomed Sci 2006;13:225-32.

8. Appendix

Abbreviations

Abbreviations	*Full Name*
α-SMA	α-smooth muscle actin
AF2	Activation function 2
ALT	Alanine-aminotransferase
AP	Apurinic/apirimidinic
APS	Ammoniumperoxodisulfat
AST	Aspartate-aminotransferase
BCL-2	B-cell lymphoma 2
BDL	Bile duct ligation
BM	Bone marrow
BMC	Bone marrow cells
BMT	Bone marrow transplant
BSA	Bovine Serum Albumin
Cat	Catalase
Ccn A	Cyclin A
Ccn D	Cyclin D
Ccn E	Cyclin E
cDNA	Complementary DNA
c-Myc	v-myc avian myelocytomatosis viral oncogene homolog
COL1A1	Collagen type I α1
DAB	3,3´-diamino benzidine
DAPI	4,6-diamino-2-phenylindole
DMEM	Dulbecco´s modified Eagle´s medium
DNA	Desoxyribonucleic acid
dNTP	Desoxyribonukleotidtrisphospate
DR	Death Domain
DTT	Dithiothreitol
Δhepa	Hepatocyte-specific knockout
EDTA	Ethylendiamintetraacetic acid
ECL	Enhanced chemiluminescence
ECM	Extracellular matrix
EGF	Epidermal growth factor
ER	Endoplasmic reticulum
ERK	Extracellular signal-regulated kinase
FACS	Fluorescence activated cell sorting
FAS	TNF receptor superfamily
Fb	Fibronectin
FCS	Fetal calf serum
FFA	Free fatty acids
FITC	Fluoresceinisothocyanat
GAPDH	Glyceraldehyde 3-phosphate dehydrogenase

GFAP	Glial Fibrillary Acidic Protein
H&E	Hematoxylin and eosin
HCC	Hepatocellular carcinoma
HCV	Hepatitis C Virus
HRP	Horseradish peroxydase
HSC	Hepatic Stellate Cells
IF	Immunofluorescence
IHC	Immunohistochemistry
ISR	Insuling receptor
JIP	JNK-interacting protein
JNK	c-Jun N-terminal kinase
KC	Kupffer cell
Ki-67	cell cycle specific protein encoded by the MKI67 gene
LMW	Low molecular weight
LPS	Lipopolysaccharide
MAPK	Mitogen-activated protein kinase
Mcl-1	Myeloid cell leukemia 1
MCP1	Monocyte chemotactic protein-1
MMP2	Matrix Metalloprotease also known as collagenase 2
Mn-SOD	Manganese superoxide dismutase
MOPS	Morpholinopropansulfon
mRNA	Messenger RNA
NAFLD	Nonalcoholic fatty liver disease
NASH	Nonalcoholic steatohepatitis
NF-kB	nuclear factor kappa-light-chain-enhancer of activated B cells
NPC	non-parenchymal cells
OD	Optical density
OPN	Osteopontin
PBS	Phosphate buffered saline
PBS-T	PBS-Tween
PCNA	Proliferating cell nuclear antigen
PCR	Polymerase chain reaction
PDGF	Platelet derived growth factor
PEST	prolin (P), Glutamic acid (E), Serine (S), Threonine (T)
PFA	Paraformaldehyde
PH	Partial hepatectomy
RANTES	regulated upon activation, normal T cell expressed and secreted
RNA	Ribonucleic acid
RPMI	Roswell Park Memorial Institute
ROS	reactive oxygen species
RT	Room temperature
SDS	Sodium dodecyl sulphate
SEC	Sinusoidal endothelial cells

Ser	Serine
SOCS	Suppressor Of Cytokine Signaling
TAE	Tris Acetate EDTA Buffer
TBS	Tris buffered saline
TBS-T	Tris buffered saline supplemented with Tween 20
TE	Tris-EDTA-Buffer
TEMED	N´,N,N´,N´-Tetramethyldiamine
TGF-beta	Transforming growth factor beta
Thr	Threonine
TIMP-1	Tissue inhibitor of metalloproteinase-1
TNF-α	tumor necrosis factor-α
Tris	2-Amino-2(hydroxymethyl)-1,3-propandiol
TUNEL	Terminal deoxynucleotidyl transferase dUTP nick end labeling
Tween 20	Polyoxyethylensorbitanmonolaureat
v/v	Volume per Volume
WT	Wild type

Publications

Teile dieser Arbeit wurden bereits vorab veröffentlicht oder zur Publikation eingereicht:

1. **Zhao G**, Hatting M, Nevzorova Y.A, Boekschoten M, Drvarov O, Roskams T, Müller M, Davis R.J, Cubero F.J, Trautwein C. (American Association of Liver Diseases, Boston, USA, 2012): JNK1 in Hepatic Stellate Cells is a crucial mediator of liver fibrogenesis. Poster. Awarded with Presidential Distinction.

2. Cubero F.J, **Zhao G**, Hatting M, Drvarov O, Sellge G, Nevzorova Y.A, Liedtke C, Trautwein C. (American Association of Liver Diseases, Boston, USA 2012): The roles of JNKs in the development of HCC. Poster.

3. Cubero F.J, **Zhao G**, Nevzorova Y.A, Hatting M, Trautwein C (European Association for the Study of Liver Disease, Barcelona, Spain, 2012): Different roles of JNK 1 and JNK2 in the development of NASH and HCC. Journal of Hepatology 2012: 56 (2):S2-S3.

4. Hatting M, Cubero F.J, **Zhao G**, Schumacher F, Sellge G, Liedtke C, Gassler N, Trautwein C. (European Association for the Study of Liver Disease, Barcelona, Spain, 2012): Modulation of hepatic fibrosis and lipid content by caspase in non-alcoholic steatohepatitis. Journal of Hepatology 2012: 56 (2): S491.

5. Cubero F.J, **Zhao G** ,Hatting M, Drvarov O, Nevzorova Y.A, Al Massoudi M, Gassler N, Liedtke C, Trautwein C. (GASL, P1.05, Hamburg, Germany, 2012): JNK1 is protective for the progression of NEMO-dependent hepatitis. Poster.

6. Cubero F.J, **Zhao G,** Hatting M, Drvarov O, Sellge G, Nevzorova Y.A, Liedtke C, Trautwein C. (American Association of Liver Diseases, San Francisco, USA, 2011): Distinct roles of JNK1 and JNK2 in the progression of chronic liver injury. Poster

7. Hatting M, Cubero F.J, Schumacher F, **Zhao G** ,Sellge G, Gassler N, Liedtke C, Trautwein C. (American Association of Liver Diseases, San Francisco, USA, 2011): Ablation of caspase-8 in hepatocytes decreases the hepatic triglyceride storage in murine models of non-alcoholic steatohepatitis. Poster.

8. Cubero F.J, **Zhao G**, Trautwein C. (2011): JNK: A Double-Edged Sword in Tumorigenesis. Hepatology, Vol. 54, No. 4, 2011, 1470-1472.

Eidesstattliche Erklärung gemäß § 5 Abs. (1) und § 10 Abs. (3) 12. der Promotionsordnung

Hiermit erkläre ich, **Herr Gang Zhao** an Eides statt, dass ich folgende in der von mir selbständig erstellten Dissertation “JNK1 in Hepatic Stellate Cells is a crucial mediator of liver fibrogenesis in mice ” dargestellten Ergebnisse erhoben habe:

Durchführung sämtlicher dargestellter Experimente, sowie deren statistische Auswertung (ggf. unter Hilfestellung der unten aufgelisteten Personen).

Bei der Durchführung der Arbeit hatte ich folgende Hilfestellungen, die in der Danksagung angegeben sind:

A. Kooperationspartner, Univ.-Prof. Dr. med. Nikolaus Gaßler, Institut der Pathologie im Universitätsklinikum Aachen: die histologischen Färbungen und die Auswertung HE und Sirius Red gefärbter Gewebeschnitte.

B. Dr. Francisco Javier Cubero: Technische Betreuung der Arbeit, Hilfestellung bei Planung von Experimenten

C. Frau Sibille Sauer-Lehnen und Frau Carmen C. Tag in Q3 Platform: Isolierung von Hepatozyten und Sternzellen.

D. Frau Malika Al Masaoudi: Anweisung für Realtime PCR und Isolierung von mRNA.

E. Doktorvater, Univ.-Prof. Dr. Christian Trautwein: Betreuung der Arbeit und Studiendesign, Korrektur der Dissertation.

Acknowledgements

To begin with, I would like to thank my family for all of their support during my lifetime.

I want to thank Prof. Dr. Christian Trautwein for the opportunity to work in the Department of Medicine III of the University Hospital RWTH Aachen offering me excellent research conditions. I am grateful for his supervision, guidance and advice during the project and throughout my studies.

Furthermore, I would like to thank Dr. Francisco Javier Cubero for all of his support and for all the constructive discussions we have had and for the possibility to perform my thesis with his strong support. I am very grateful for his friendship and generous help from the beginning of my study in Germany.

A very special thanks goes to Prof. Dr. Ralf Weiskirchen for accepting to supervise my thesis and for his additional contributions during the revision. To Prof. Dr. med. Nikolaus Gaßler, thank you very much for being so kind to revise my thesis.

Thanks goes to the excellent assistance of Frau Sibille Sauer-Lehnen, Frau Carmen C. Tag and the Core Unit “Q3 - Cell Isolation” of the SFB/TRR57 with the isolation of primary hepatic stellate cells as well as helpful advice.

Thanks to Dr. Yulia A. Nevzorova for her great help and for the commitment, interesting discussions and ideas while preparing my thesis.

Thanks to my co-workers Dr. Maximilian Hatting and Dr. Oliver Drvarov from the group who were a great help to me and who made coming to work a pleasure. In particular, I want to mention Malika for her excellent experimental and technical support.

For all the good times I had during my work and after work I want to thank Wei Hu, Jin Peng, Haksier, Sara, and the rest of members of the Laboratories within Department of Medicine III.

I want to also thank all the animal caretakers, especially Frau Birgit Müller for the support and care of my animal lines which contributed greatly to this work.

A big thanks to all current and former colleagues at the Klinikum, for the friendly atmosphere, support, coffee breaks and nights-out, which made working so much more fun.

Erklärung § 5 Abs. 1 zur Datenaufbewahrung

Hiermit erkläre ich, dass die dieser Dissertation zu Grunde liegenden Originaldaten

- bei meinem Betreuer, ***Univ.-Prof. Dr*** .**Christian Trautwein*, Med. Klinik III***, des Universitätsklinikums Aachen,

hinterlegt sind.

Curriculum Vitae

Personal Data

Surname, Name	Zhao, Gang
Street	Kullenhof Str. 54B
ZIP-code, City	52074 Aachen
Date of Birth	08.12.1972
Place of Birth	Anhui
Nationality	China

Education:

9/2002–7/2005	Genetics Research Center, Southeast University and Clinic Southeast University, Nanjing, 210009, P.R. of China
9/1988 – 8/1991	Anhui Medical College, Hefei, Anhui province, P. R. of China

Working Experience:

11/2009 – present	Department of Internal Medicine III, University Hospital, RWTH, Aachen, 52074, Germany.
8/2005 –10/2009	Department of Liver and Biliary-Tract, Zhongda Hospital, Southeast University, Nanjing 210009, P.R. of China
9/1991– 9/2002	Department of Surgery, Magang Hospital, Ma-anshan, 243000, P.R. of China